Organotypic Skin Model

Jan Řezníček

Bachelor's thesis
2023

Tomas Bata University in Zlín
Faculty of Technology

Univerzita Tomáše Bati ve Zlíně
Fakulta technologická
Ústav technologie tuků, tenzidů a kosmetiky

Akademický rok: 2022/2023

ZADÁNÍ BAKALÁŘSKÉ PRÁCE

(projektu, uměleckého díla, uměleckého výkonu)

Jméno a příjmení:	**Jan Řezníček**
Osobní číslo:	**T200037**
Studijní program:	**B0711A130009 Materiály a technologie**
Specializace:	**Biomateriály a kosmetika**
Forma studia:	**Prezenční**
Téma práce:	**Organotypický model kůže**

Zásady pro vypracování

I. Teoretická část:
Student vypracuje literární rešerši na danou problematiku a osvojí si základní techniky práce v laboratoři buněčné biologie.
II. Praktická část:
V rámci praktické části tématu bude provedena příprava organotypického modelu kůže založena na *in vitro* kokultivaci neonatálních keratinocytů s dermálními fibroblasty na kolagenovém základu.

Forma zpracování bakalářské práce: **tištěná/elektronická**
Jazyk zpracování: **Angličtina**

Seznam doporučené literatury:

[1] SNUSTAD, D. Peter, SIMMONS, J. Michael, 2017. *Genetika*. Masarykova univerzita, Brno. ISBN: 978-80-210-8613-5.
[2] ALBERTS, B., *et al.*, 2014. *Molecular Biology of the Cell. Sixth Edition*. W. W. Norton & Company. ISBN: 978-0-8153--4464-3.
[3] Stark, H. J. *et al.* 2004. Organotypic co-cultures as skin equivalents: A complex and sophisticated in vitro system. *Biological Procedures Online*. (6): 55-60. doi: 10.1251/bpo72.
[4] Won Oh, J., *et al.* 2013. Organotypic Skin Culture. *Journal of Investigative Dermatology* 133(11): e14. doi:10.1038/jid.2013.387.
[5] Owczarzy A., *et al.* 2020. Collagen – structure, properties and applications. *Engineering of Biomaterials* (156):17–23. https://doi.org/10.34821/eng.biomat.156.2020.17-23.

Vedoucí bakalářské práce: **Ing. Kristýna Valášková**
Ústav technologie tuků, tenzidů a kosmetiky

Datum zadání bakalářské práce: **1. února 2023**
Termín odevzdání bakalářské práce: **19. května 2023**

L.S.

prof. Ing. Roman Čermák, Ph.D.
děkan

doc. Ing. Marián Lehocký, Ph.D.
ředitel ústavu

PROHLÁŠENÍ AUTORA
BAKALÁŘSKÉ PRÁCE

Beru na vědomí, že:

- bakalářská práce bude uložena v elektronické podobě v univerzitním informačním systému a dostupná k nahlédnutí;
- na moji bakalářskou práci se plně vztahuje zákon č. 121/2000 Sb. o právu autorském, o právech souvisejících s právem autorským a o změně některých zákonů (autorský zákon) ve znění pozdějších právních předpisů, zejm. § 35 odst. 3;
- podle § 60 odst. 1 autorského zákona má Univerzita Tomáše Bati ve Zlíně právo na uzavření licenční smlouvy o užití školního díla v rozsahu § 12 odst. 4 autorského zákona;
- podle § 60 odst. 2 a 3 autorského zákona mohu užít své dílo – bakalářskou práci nebo poskytnout licenci k jejímu využití jen s předchozím písemným souhlasem Univerzity Tomáše Bati ve Zlíně, která je oprávněna v takovém případě ode mne požadovat přiměřený příspěvek na úhradu nákladů, které byly Univerzitou Tomáše Bati ve Zlíně na vytvoření díla vynaloženy (až do jejich skutečné výše);
- pokud bylo k vypracování bakalářské práce využito softwaru poskytnutého Univerzitou Tomáše Bati ve Zlíně nebo jinými subjekty pouze ke studijním a výzkumným účelům (tj. k nekomerčnímu využití), nelze výsledky bakalářské práce využít ke komerčním účelům;
- pokud je výstupem bakalářské práce jakýkoliv softwarový produkt, považují se za součást práce rovněž i zdrojové kódy, popř. soubory, ze kterých se projekt skládá. Neodevzdání této součásti může být důvodem k neobhájení práce.

Prohlašuji,

- že jsem na bakalářské práci pracoval samostatně a použitou literaturu jsem citoval. V případě publikace výsledků budu uveden jako spoluautor.
- že odevzdaná verze bakalářské práce a verze elektronická nahraná do IS/STAG jsou obsahově totožné.

Ve Zlíně, dne:

Jméno a příjmení studenta:

.....
podpis studenta

ABSTRAKT

Teoretická část bakalářské práce se zabývá základním anatomickým popisem lidské kůže a jejím složením. V práci jsou charakterizovány hlavní buňky dermis i epidermis, produkty jejich metabolické aktivity, a jejich vliv na funkce kůže. Dále je pozornost věnována tkáňovému inženýrství kůže a kožním modelům, které napodobují strukturu kůže a slouží jako alternativa k testování na zvířecích modelech *in vivo*. Praktická část se poté zabývá popisem a provedením analytických metod pro charakterizaci chování buněčné linie v různých experimentálních podmínkách. Na buněčné linii NIH/3T3 byla za běžných podmínek kultivace stanovena růstová křivka, dále se sledovalo jejich chování v různých koncentracích kolagenu typu I pomocí *in vitro* scratch assay. Poznatky z těchto metod byly využity k přípravě trojrozměrného (3D) organotypického modelu kůže založené na kokultivaci neonatálních keratinocytů s dermálními fibroblasty na kolagenovém základu.

Klíčová slova: kůže, kolagen, tkáňové inženýrství, modely kůže, růstová křivka, scratch assay

ABSTRACT

The theoretical part of the bachelor's thesis describes the basic anatomy of human skin and its composition. This work characterizes the main cells of the dermis and epidermis together with the products of their metabolic activity and influence on skin functions. Furthermore, attention is paid to tissue engineering of the skin and skin models that mimic the native skin and serve as an alternative to testing on animal models *in vivo*. The practical part then describes and implements analytical methods for characterizing the behavior of the cell line in various experimental conditions. Under normal cultivation conditions, a growth curve was constructed for NIH/3T3 cell line. Additionally, their behavior in different concentrations of type I collagen was monitored using an *in vitro* scratch assay. Knowledge from these methods was used in the preparation of a three-dimensional (3D) organotypic skin model based on the co-cultivation of neonatal keratinocytes with dermal fibroblasts on a collagen base.

Keywords: skin, collagen, tissue engineering, skin models, growth curve, scratch assay

I would like to express my deepest appreciation to the supervisor of my Bachelor's thesis, Ing. Kristýna Valášková, for invaluable guidance, advice, patience, and time dedicated to my work. This academic work would also not be possible without prof. Ing. Petr Humpolíček, Ph. D., who helped me with choosing the topic of my thesis and allowed me to start working on the practice during the summer break.

I would like to extend my sincere thanks to my classmates, who have kept my spirits and motivation high throughout the school years. I am also grateful to my family, friends, and my partner, who supported me during this journey and believed in me, and most importantly, were patient with me.

I hereby declare that the print version of my Bachelor's thesis and the electronic version of my thesis deposited in the IS/STAG system are identical.

CONTENTS

INTRODUCTION

At the end of the last century, a rather peculiar photograph stormed the world. In it was a bald laboratory mouse with what appeared to be a human ear growing from its back [1]. However, the ear-like structure was "merely" a tissue-engineered cartilage in the shape of a human ear. Vacanti et al. seeded bovine chondrocytes onto a synthetic and biodegradable polymer and implanted it in immunologically incompetent mice. It was a demonstration of the possibility to take a biomaterial of choice, seed it with appropriate cells and implant it into a biological system to generate new tissue [2]. Back then, this photograph became quite controversial and mistakenly assumed to be the case of genetic engineering, or mad scientists "playing god" [3]. In truth, this was but a case of tissue engineering (TE) that has gone viral due to its shocking nature.

Nonetheless, the field of TE has immensely progressed since then due to clinical demand for new tissues caused by donor shortage. Not only that, but TE promises to generate organotypic substitutes of parts of the human body *in vitro* which could help eliminate the need for testing on animals. One such organ is the skin. Advances in recreating the first skin *in vitro* were made about 20 years prior to the Vacanti mouse experiment. In the 1980s, the first patent for a "living skin equivalent" was introduced by coculturing the major cells of the skin on a collagen lattice. This formed the basis for the first commercially available skin equivalent in the early 1990s. [4].

The skin is the first barrier against environmental harm to the mammalian body. It represents many aspects of protection, but also communication of the "inside" world with the "outside" world [5]. When it is damaged, such functions cannot be fulfilled, and that puts the body at risk of further harm. The body has its resolutions for restoring the skin's protective function, however, certain injuries, such as acute burns, can be too extensive. In these cases, the body's natural ability to regenerate properly ceases in efficacy. For this reason, humans have employed many creative strategies to promote the healing of extensive damage that mainly requires donor tissue, which is ultimately a limitation of these methods. TE has introduced new solutions which partially solve the need for donor sites at the clinic. Additionally, the engineering of skin tissue has extended into the laboratory, where established 3D skin equivalents help in studying the skin's structure, physiology, and response to applied active compounds [6; 7].

I. THEORY

1 ANATOMY OF THE HUMAN SKIN

The skin is an extensive organ covering the body, making up its outermost layer. As it covers nearly 2 m^2 in adults on average, it is considered one of the largest organs of the human body. Its thickness varies significantly over all parts of the body. For example, the skin of the back is the thickest, whereas the skin of the eyelids is the thinnest [8]. As for its weight, it makes up about 8-10% of body mass [5]. The skin structure consists of two main layers: the outer layer, the epidermis, and the inner layer, the dermis [9]. Beneath the dermis lies the hypodermis, which is made up of adipose tissue. The layers of the skin vary significantly in their anatomy and function [10].

The structure of the skin allows for its important functions. It is the first line of protection against physical, chemical, and biological harm, thus making up the barrier function of the body. This is also related to the skin's "self-cleaning" ability, as the epidermis can dispose of foreign bodies in the process of continual desquamation. The skin secretes sweat, sebum, keratin, and melanin [5]. Sweat, produced by the sweat glands, plays a role in thermoregulation by evaporation. The ability of the skin to either widen or narrow blood vessels and the fact that it is a bad heat conductor, is another component of its thermoregulatory function [8]. Sebum, produced by the sebaceous glands, mainly consists of fatty acids and squalene. It mixes with lipids naturally present in the epidermis and sweat to cover the skin in the protective film with a slightly acidic pH of 5-6. This film, also called the acid mantle, has antimicrobial properties. Keratin is a protein produced when keratinocytes in the epidermis differentiate, and it is the strongest structure of the human organism. Melanin is a pigment synthesized by melanocytes and has a photoprotective function [5]. The skin shields our bodies from the outside antigens and contains immunocompetent cells, and as such is part of the immune system [8].

Aside from the above-mentioned functions, the skin is also a sensory organ. Various receptors mediate information between the external and internal environment, like pain, pressure, touch, or the change in temperature. Its role in psychosocial relationships is not negligible either, as the appearance of one's skin can influence the perception of an individual in human society [5].

1.1 Epidermis, dermis, hypodermis

The epidermis is the superficial, avascular layer of the skin, consisting of epithelium originating from the ectoderm. Besides keratinocytes that make up most of the epidermis,

other cells present in the epidermis are Merkel cells, melanocytes and Langerhans cells [8]. The epidermis is divided into several distinct histological layers that are made up of keratinocytes in different stages of development. The deepest epidermal layer consists of cells that are connected to the basement membrane, an interface separating the epidermal and dermal layers [5].

The dermis is a fibrous layer of the skin located beneath the epidermis. It accounts for most of the skin mass and for the skin's physical strength, due to the high presence of collagen and elastic fibers. Here, three main types of cells are present: fibroblasts, histiocytes, and mastocytes. The dermis is split into two parts: *stratum papillare*, or papillary dermis, and *stratum reticulare*, or reticular dermis. The papillary dermis is a superficial, thin part of the dermis and lies adjacent to the epidermis. It contains loose fibers of collagen and elastin that spread widely across the papillary dermis, but more connective tissue cells when compared to the reticular dermis. Additionally, blood and lymphatic vessels found throughout this part provide nutrition and drainage of the waste to the skin respectively [9]. As seen in **Figure 1**, this layer arises against the epidermis by heightened papillae, increasing the contact area at the junction of the two layers. The "interlocking" of the dermal and epidermal layers gives integrity to the skin and is more pronounced in the areas that need to withstand great friction, such as hands and feet [10]. The reticular dermis is the lower part of the dermis. Here, denser bundles of collagen and elastic fibers intertwine and form a complex structure, giving the skin physical strength and elasticity to withstand mechanical stress. Skin appendages, such as sweat and oil glands along with hair follicles, are present in the reticular dermis [9].

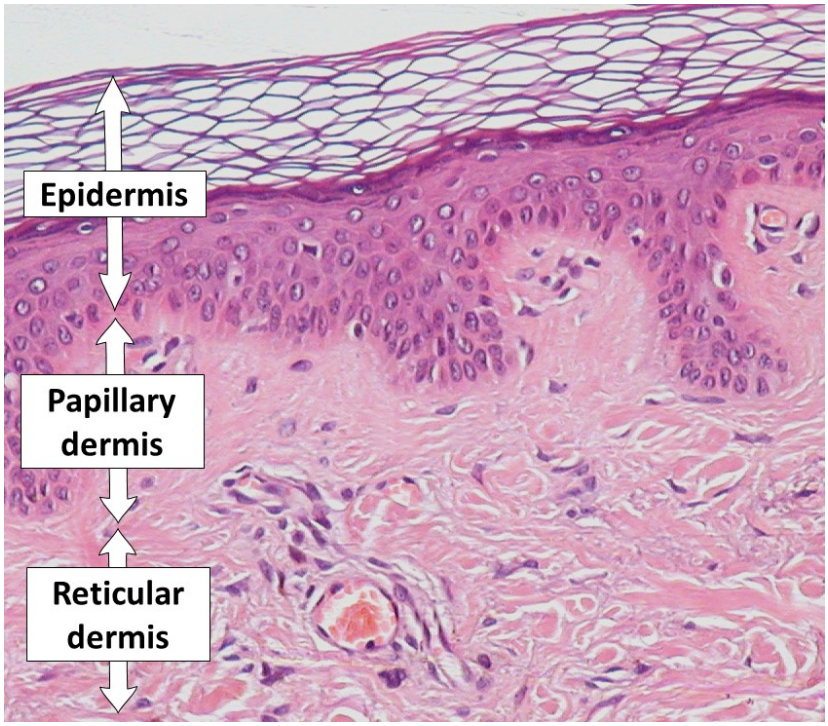

Figure 1: Histology of the epidermis and layers of the dermis: papillary dermis and reticular dermis. Available from [11].

Beneath the dermis lies a layer of mainly loose connective and adipose tissue, the hypodermis. It connects the dermis to the superficial fascia and periosteum by a network of collagenous fibers known as the *reticanula cutis* [12]. The common types of cells in the hypodermis are fibroblasts and adipocytes [13]. As shown in **Figure 2**, nerves and blood vessels weave throughout. The importance of this layer lies in insulation properties and mechanical protection provided by the subcutaneous tissue [8]. The hypodermis can also

affect keratinocyte and fibroblast proliferation, influencing wound healing and proliferation, therefore affecting the layers above [14].

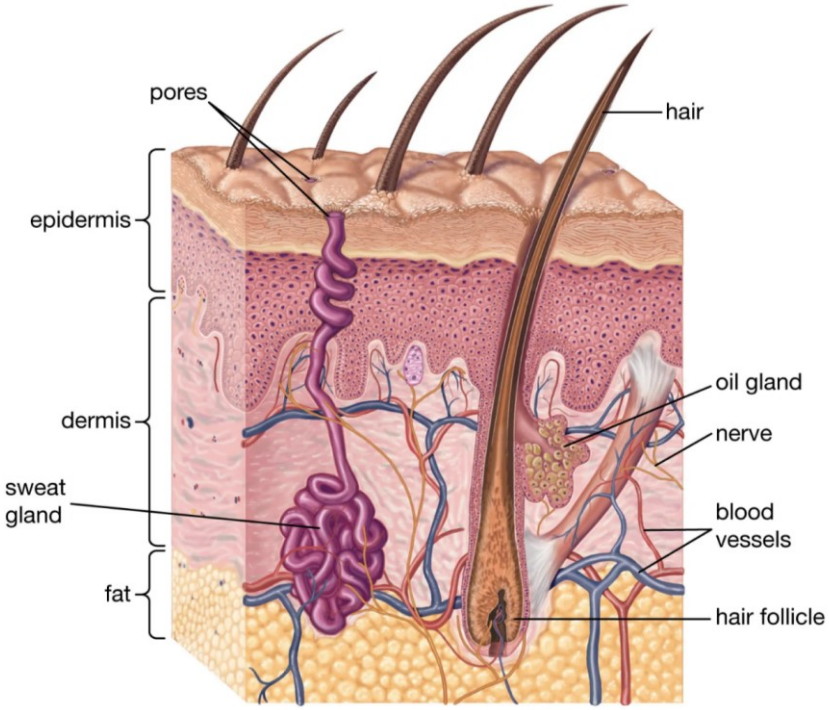

Figure 2: Anatomy of the skin. Available from [15].

1.2 The role of fibroblasts and keratinocytes for skin function

As it was already mentioned, keratinocytes are the main cells of the epidermis and dictate its structure. These cells go through development and make up five distinct histological layers, their order from top to bottom is: *stratum corneum*, *stratum lucidum*, *stratum granulosum*, *stratum spinosum* and *stratum basale* [9]. The aforementioned layers are pictured in **Figure 3** below.

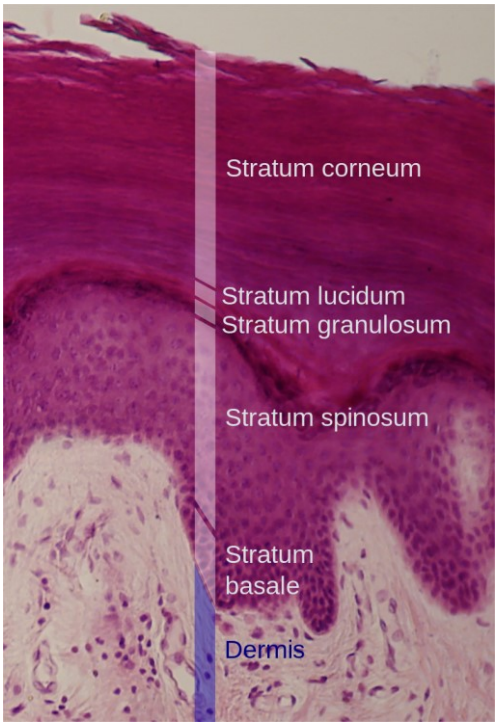

Figure 3: Histology of the epidermis showing its layers. Available from [16].

The *Stratum basale* is the deepest layer of the epidermis. It consists of a sheet of keratinocytes that are columnar in shape. The cells are connected by desmosomes, and the connection to the basement membrane is secured by hemidesmosomes [5]. The cells undergo mitosis, during which they migrate upwards into the *stratum spinosum*. This layer consists of a few rows of keratinocytes, flattened into a polyhedral shape. The cells in the lower rows proliferate, whereas the cells in the upper rows lose this ability and begin to differentiate instead [5; 8]. The next layer is the *stratum granulosum*, consisting of flattening keratinocytes. The typical characteristic of the cells in this layer are grains of keratohyalin, which is an intermediate of keratin, in their cytoplasmatic membrane. These grains consist of profilaggrin and other proteins that contribute to the process of cornification. As the cells are moved toward the top layer, profilaggrin will transform into filaggrin, which will help bundle up keratin fibers [5; 10]. Here, keratinocytes form a cornified hard shell around their cytoplasmatic membrane and undergo programmed cell death soon after. At some point, the dead keratinocytes lose their nucleus and become the *stratum lucidum*, named after its transparent appearance [10]. The keratin fibers are formed in this layer. The final stop of the keratinocytes' journey is the *stratum corneum*, the outermost epidermal layer [9]. By the time the keratinocytes reach this layer, they have transformed into flat, nucleus-free, cornified versions of themselves, referred to as corneocytes. The cells here are densely stacked on top of each other [5]. The upper part of this layer regularly separates into smaller

pieces and then peels off; therefore, it is called the *stratum disjunctum*. The lower part of this layer keeps together and is called the *stratum conjunctum* [8]. For the major part, corneocytes contain mainly keratin and lipids. Moreover, keratin fibers can be found in the extracellular matrix (ECM) where they connect the cells together. The keratin and lipid content of *stratum corneum* prevents water loss through the epidermis by evaporation and defends the organism against penetration of undesirable outside substances [5; 8; 9; 10].

Meanwhile, the dermis has a fibrous structure largely determined by the dermal fibroblasts that reside in this layer. These cells are an active form of fibrocytes that secrete components of ECM while also organizing this structure. The components produced by fibroblasts are proteins that form fibers thanks to their structure. These fibers are "woven" through the dermal layer and ensure its exceptional mechanical properties [5; 9; 17; 18; 19]. Fibroblasts mainly produce collagen fibers of type I; however, other collagen types are also present [17; 19]. Collagens are divided into two groups: nonfibrillar collagens and fibrillar collagens, where collagen I belongs to [20]. The fibers of collagen I run parallel to the skin's surface and ensure resistance against stretching in all directions. Collagen's I ability to give the skin such property is derived from its hierarchical structure [5; 9]. One fiber of collagen I consists of many fibrils that are made up of microfibrils [9]. These microfibrils are also called the tropocollagen and they are a basic structural unit of collagen. It is an α-helix left-handed molecule that is composed of three polypeptide chains that spirally wrap around each other due to electrostatic and hydrophobic bonds. On the atomic level, a single polypeptide chain is composed of amino acids. Out of all the amino acid content of collagen, most is taken up by Glycine (Gly) and Proline (Pro) which ensure the formation and cohesion of the tropocollagen by creating Gly-Pro hydrogen bonds. Another amino acid, Hydroxyproline (Hyp), also plays an important role in collagen fiber formation [9; 19; 20; 21]. Aside from the mechanical properties of collagen, it can also affect fibroblast cell behavior through cells' membrane receptors, regulating their migration and proliferation [20].

Another structurally important product of fibroblast activity is elastin [5]. This protein, like collagen, forms fibers that spread throughout the dermis and provide stretch and elastic recoil properties to the skin. At present, the structure of the elastic fiber and the basis of its reversible elasticity have not been fully defined [9; 22]. However, it is known that an elastic fiber mainly consists of elastin at its core, a polymer with a monomeric precursor tropoelastin (TEl). This monomer is by itself soluble in water, but it self-assembles into insoluble fibers by self-association through hydrophobic domains and by cross-linking by desmosine, an

amino acid only present in elastic fibers composed of lysin residues [22; 23]. TEl has hydrophilic regions with abundance of Alanine (Ala) and Lysine (Ly). Lysyl oxidase targets these amino acids for the cross-linking. The hydrophobic regions of TEl are rich in Gly, Pro and Valine (Val). The result is a network that is thought to distribute mechanical stress across itself and give the skin elastic properties [22; 24]. The rest of what makes up an elastic fiber is a microfibrillar structure, which contains components that include fibrillins, fibulins and microfibril-associated glycoproteins. These microfibrils surround the core of the elastic molecule and together they form an elastic fiber [9; 23].

Aside from collagen and elastin, fibroblasts' metabolic activity also produces glycosaminoglycans (GAGs), which are polysaccharides. An example of GAGs is hyaluronic acid and dermatan sulphate. They combine with proteins to form hydrophilic proteoglycans that aid the skin by maintaining proper moisture content and provide support for other components of the dermis [9; 19]. Importantly, proteoglycans in the dermis are a part of a so-called "ground substance", a viscoelastic solgel that is involved in water binding and flow resistance. Collagen and elastic fibers lie in this matrix and together they ensure the integrity of the skin [9; 10].

2 TISSUE ENGINEERING

The formal definition of TE has different variations of the same definition. The following one was proposed by one of the founding scientists of this field, Robert Langer: "*TE is an interdisciplinary field that applies the principles of engineering and life sciences toward the development of biological substitutes that restore, maintain, or improve tissue function or a whole organ*" [4]. Per this definition, TE is based on principles of cell transplantation, materials science, and bioengineering. This field combines them with the intention to find restore or improve tissue's anatomy and function or guide the development of new patient-specific tissue or an organ. It finds use in medicine due to limitations of organ transplantation, such as the lack of suitable organ transplants for the patient in question [25; 26]. The strategies of TE can be divided into two categories: Scaffold-based and scaffold-free. Scaffold-based approaches encompass the use of scaffolds to affect the differentiation, adhesion, or viability of the cells. Their topography, chemistry, and even fabrication methods are important factors that influence the behavior of implanted cells. On the other hand, scaffold-free approaches use direct administration of cells. The cells can be co-applied with growth factors to improve efficacy and affect cell viability, differentiation, migration, and proliferation [26].

The materials used in TE are called biomaterials. Those can be polymers, ceramics, composites, or metals. Biomaterials can be used either as scaffolds or carriers and need to have controlled surface chemistry, mechanical structure, porosity, and degradability, all with regards to the respective application. Depending on the location, TE can be also classified as *in vivo* or *in vitro*. The former relies on cooperation with the body's natural ability to regenerate by local delivery of cells, growth factors, or biomaterials to guide regeneration. The latter work outside the body in the laboratory, where cells are cultured and guided towards the formation of new tissue before being transplanted. Nowadays, TE has branched into the engineering of several tissues or organs, such as the skin, skeletal system, vascular system, or nervous system [4; 25].

2.1 Tissue engineering of the skin tissue

As it has been mentioned in **Chapter 1**, the skin has a fundamental role in the protection of the body against harm in the form of injuries, ultraviolet radiation, and pathogens. When the skin is injured, its components participate in the healing process. However, certain wounds, such as extensive burns, can cover a large surface area and in such cases, the natural

regeneration ability of the body seems to cease in efficacy with the results being irreversible scarring that lacks the healthy skin's physiological functions. Importantly, extensive damage may be fatal. Due to advancements in TE, successful efforts have been made to create substitutes of human skin both cellular (cell-based) and acellular (cell-free) that aid not only in clinical applications but also in research. [27; 28; 29; 30]. Currently, there are commercially available tissue-engineered skin equivalents that can be divided into the following main groups: epidermal, dermal, and dermo-epidermal or composite [29]. While engineering the skin tissue, it is crucial to maintain the used cells' normal phenotype and functionality while obtaining enough cells to generate a skin substitute suitable for *in vivo* and *in vitro* applications [7].

2.1.1 *In vivo* applications

The skin can become damaged due to various reasons, resulting in acute trauma, such as burn wounds, and chronic trauma, such as diabetic ulcers, which heal slowly [4]. Usually, a cascade of events starting with an immune response leads to new tissue matrix generation by fibroblasts in the wound site, followed by migration of keratinocytes from the edges of the wound. Finally, this leads to re-epithelialization and revascularization of the wound. However, some wounds can be too extensive, they reach up to the dermis and do not allow for the re-epithelialization to take place. In such cases, wound healing is delayed and often results in scar tissue formation [29]. Many strategies have been developed to treat the damaged site. They can be divided into conventional approaches that have been applied in clinical practice for hundreds of years and new, modern approaches [6; 7].

Conventional strategies employ skin grafts to regenerate the wound. These techniques rely on a donor site of skin either from the patient's own tissue (autograft), other patients (allograft), or other species (xenograft) [6]. For autografts, a layer of skin with epidermis and a portion of the dermis is shaved from the donor site using a dermatome and placed on the wound site. The thickness of the dermal layer determines the healing quality [29]. The donor site can be harvested few times more, however, that can lead to scarring [7]. Because the donor skin comes from the patient's own tissue, autographs present no risk of rejection [6]. If the wound covers a large area of the body, autographs cannot be employed due to lack of the patient's own donor sites. In these cases, skin allographs can be used. The donor skin usually comes from a cadaver but may also come from a living patient [6]. Skin allografts provide a temporary solution due to immunogenic rejection by its host. They provide cover to the wound area and promote the production of compounds that aid in wound healing;

however, safety issues arise due to the risk of viral transmission [7; 29]. Xenografts, too, provide temporary coverage. This approach uses collagen derived from other species that is deposited onto the wound, where it can get absorbed as the wound heals [6].

Modern strategies encompass a wide array of methods that include cell-based and cell-free designs that both elicit only low immunogenic response [29]. In general, cell-based skin substitutes are more expensive than their cell-free counterparts and they also require long cell culture period to manufacture [30]. Cell-free substitutes of human skin have main use in clinical applications where they work as a protection against harm from the outer environment and loss of fluid, deliver agents to support the wound healing process, and promote proliferation. Those can be acellular matrices, meshes, and membranes made of biomacromolecules that mimic the microenvironment of the ECM, and similarly designed synthetic and composite materials. Acellular substitutes may be used either temporarily or permanently and there is also a possibility to use them along with skin autographs [7; 29; 30]. Cell-based designs of human skin substitutes follow a more complicated path, often consisting of a scaffold layer that is seeded with cells. The cells used in developing such substitutes naturally involve those present in the skin, the epidermal keratinocytes, and the dermal fibroblasts. They can be autologous or allogeneic. Autologous skin substitutes use cells derived from the same patient by skin biopsy. Allogeneic skin substitutes consist of cells obtained from other donors, mainly from neonatal foreskins. With this approach, epidermal, dermal, and dermo-epidermal skin substitutes can be prepared with respect to the desired application. They can be simple membranes or complex 3D full-thickness models that can promote proliferation, differentiation and finally re-epithelialization in the wound site and aid in research [6; 29; 31].

2.1.2 *In vitro* applications

Tissue engineered human skin has been well developed to biologically mimic natural skin, making its use possible for *in vivo* applications, as discussed earlier. However, tissue engineered skin also finds use as an alternative to animal testing or two-dimensional (2D) *in vitro* cell cultures in laboratory [7].

2D monolayer models are commonly used for initial toxicity screening. They are simple, quick and cheap and provide understanding of toxicity at the molecular level [7]. However, they fail to mimic the architecture of 3D tissues and there is also lack of complex cell-cell and cell-ECM interactions that are experienced *in vivo*. Cells cultured on tissue plastics also

express different characteristics to cells cultured in 3D environment, such as different morphology, uniform cell cycle, faster proliferation and higher sensitivity to active agents [32]. Therefore, they cannot reliably predict the *in vivo* effects of the tested chemical compounds [7; 32].

Toxicological assessment on 2D *in vitro* cultures usually precedes *in vivo* testing on animals [32]. While testing on animals is in certain cases useful, they ultimately suffer from several limitations. The most apparent one is the difference in metabolism, anatomical structure, and different responses to external stimuli. While mammals' tissues are, in general, similar, it does not mean that test results will be relevant and reliable for humans [33]. For example, animal models, like the Draize test, offer inadequate accuracy in predicting irritation of the human skin [4]. Another disadvantage of the use of animals in research is in the expenses for housing and breeding. Moreover, the use of animals in research also poses valid ethical questions [33]. Recently, in 2009, the European Union introduced a regulation that banned testing final cosmetic products on animals, which has, even more, fueled the market demand for an adequately engineered 3D human skin equivalent [4; 7].

Tissue-engineered 3D skin equivalent can overcome the drawbacks of 2D cultures and animal tests by being derived from human cells and sharing a similar structure to natural skin. Their great advantage is that their composition is easily controllable in laboratory conditions and can be therefore tailored to specific applications to yield the most reliable data [34]. For example, thanks to studies on 3D skin equivalents, the role of keratinocyte-fibroblast interactions on the formation of the basement membrane has been demonstrated [35]. Moreover, skin equivalents with different pathological conditions have been established to help us understand different diseases [36]. There are, for example, psoriasis skin models, that can be prepared by isolating dermal and epidermal cells from patients with psoriasis. One such model displayed that fibroblasts of psoriatic patients induce the hyper-proliferation of keratinocytes. Another discovery made real thanks to these models was that drugs targeting the cells of the immune system slow the disease [7]. Aside from psoriasis skin models, melanoma, atopic dermatitis, bacterially infected models and models reflecting *in vivo* aged skin have been established and studied [7; 37; 38]. Moreover, tissue-engineered 3D skin can also be used to study toxic properties of chemical compounds on human skin, therefore having use in drug and cosmetics development as well as other consumer goods [4].

3 IN VITRO SKIN MODELS

Clinical demand for the treatment of acute and chronic wounds has fueled the advancement in the preparation of human skin models *in vitro*. Nowadays, the preparation of *in vitro* skin models generally involves cocultivation of human dermal and epidermal cells on components of ECM to design 3D human skin equivalents. However, the development in this area started only in the late last century with "simple" epidermal substitutes and escalated into many types of skin substitutes that are available today [4; 28].

3.1 Historic overview and established skin models

A major step forward in the development was in the middle of the 1970s when Rheinwald and Green discovered that human epidermal cells proliferate under the same conditions as mouse teratoma cells. They employed a feeder layer of lethally irradiated 3T3 murine fibroblasts that contributed to the rapid growth of keratinocytes [4]. This way, the first type of an epidermal substitute was developed and termed "cultured epidermal autograft" (CEA) [29]. The technique allowed to take an epidermal skin graft and expand it without the presence of human dermal fibroblasts in a monolayer in a tissue culture flask 500 times within 3-4 weeks [28]. Naturally, they were quickly utilized in the clinic for the treatment of extensive burn injuries and chronic wounds [4]. The CEA, when transplanted, forms an epidermis, and promotes the creation of new tissue. Their advantages are in the reduction of the requirement for donor sites, and they also provide fast coverage of an injury [39]. While this sounds ideal, CEAs also suffered many drawbacks, such as blistering, scarring, wound contraction, and high cost [25; 40]. This method was later improved by employing a dermal component, an allogeneic skin graft, before CEA application [39]. The first commercially available CEA was a product named Epicel™, which is composed of sheets of autologous keratinocytes on a petrolatum gauze that is removed one week after transplantation. It is primarily used as a temporary coverage in patients with burn injuries and in patients with large congenital nevus [29].

The keratinocyte monolayer cultures quickly progressed into the development of 3D living skin equivalents. In the year 1981, a dermo-epidermal skin model, also termed full-thickness skin equivalent, was developed by Bell et al. via seeding fibroblasts on a lattice of bovine collagen type I to create a structure similar to the dermis, which is later seeded with keratinocytes and cultured at an air-liquid interface (ALI) [4; 25]. Such structure then closely resembles the native human skin. Today, this model is commercially available as Apligraf®

[28]. This product employs allogeneic cells derived from neonatal foreskins. It is used to treat chronic wounds, such as diabetic food venous leg ulcers, however, it was also used to treat patients with epidermolysis bullosa [4; 39]. One major advantage of this product is its easy application, as it does not require a surgical procedure that leaves a donor site wound. The disadvantage is a short shelf life of 5 days and, much like Epicel®, high cost [39; 40].

In the 1980s, another major step was conducted by Yannas et al. thanks to the development of the earliest dermal substitute [29; 39]. This skin substitute was unlike any other back then, as it was completely artificial and cell-free. The collagen lattice developed by Bell et al. was modified to include GAGs, predominantly chondroitin-6-sulphate, which improved the mechanical properties of the collagen matrix, biochemical stability, and allowed better control of pore structures. This was later improved upon by Boyce et al. and developed into a commercially marketed product known as Integra® [4; 25]. This product has an epidermal layer with a silicone polymer, which provides temporary coverage of the wound until a new dermis is developed. Then, it is replaced with an autograft [39]. The product has been successfully used to treat burns and chronic wounds; however, it is prone to infection, and the graft may be lost due to poor adhesion [4; 29]. Cost-wise, it fares better when compared to Epicel® and Apligraf® [40].

Since then, the field of skin tissue engineering has rapidly progressed. Nowadays, many more epidermal, dermal, and dermo-epidermal skin models are commercially available. They were summarized in **Table 1** below.

Table 1: Overview of commercially available skin substitutes

Type	Commercial product	Description	References
Epidermal	Epicel®	Autologous CAE attached to petrolatum gauze	[29]
	Epidex™	Autologous CAE, keratinocytes from cells of the outer root sheet of the patient's hair follicle	[28]
	MySkin™	Autologous keratinocytes seeded on a synthetic silicone on a support layer of silicone	[6]
Dermal	Alloderm®	Allogeneic acellular dermal matrix with intact basement membrane complex	[4]
	Biobrane®	Acellular substitute constituted of a nylon mesh, porcine collagen type I peptides with silicone film as an epidermal analog	[29; 40]
	Integra®	Acellular dermal regeneration template of bovine collagen type I and GAGs with a silicone epidermal layer	[25; 29]
Dermo-epidermal	Apligraf®	Bovine collagen type I matrix seeded with allogeneic cells from neonatal foreskins	[6]
	PolyActive	Synthetic polyethylene oxide polybutylene terephthalates scaffold seeded with autologous cells	[25]
	OrCel®	Bovine type I collagen sponge seeded with allogeneic cells from neonatal foreskins on the opposite sides	[29]

3.2 Skin equivalents

Human skin equivalent (HSE), also termed reconstructed human skin or an organotypic skin model, is a full-thickness *in vitro* skin model which has both dermal and epidermal components [4; 41]. A schematic representation of culturing HSEs is shown in the **Figure 4**. In step A, a 3D dermal matrix made of ECM components and dermal fibroblasts is prepared and submerged in the culture medium in a cell culture insert. Step B takes place after about one week; keratinocytes are seeded on top of the dermal matrix. In step C, the inserts are lifted above the surface of the medium and exposed to air, which induces differentiation of keratinocytes. In step D, the model has developed an epidermal layer after several days of being exposed to air. At this point, the skin equivalent can be harvested [35].

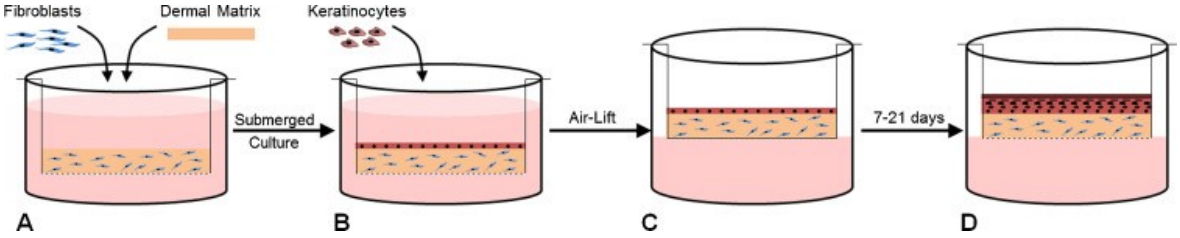

Figure 4: Schematic representation of preparing an organotypic skin model. Available from [35].

Several organ-like (organotypic) culture systems (OCSs) have been established to reconstruct human skin in *vitro*. Unlike traditional cultures, where cells quickly lose their *in vivo* properties, the cells in OCSs keep their normal physiology and function. Thanks to this ability, they can reconstruct complex tissues by engaging in intricate behaviors, such as coordinated cell division, migration, and differentiation. With that in question, employing OCSs allows for the proper generation of native-like *in vitro* skin [31; 36].

For the reconstruction of the dermis, a 3D matrix made of components of the dermal ECM is employed. Several compounds naturally present in the ECM have been utilized, such as fibrin, collagen-GAGs, or type I collagen, which has been used most widely [35; 41]. In most cases, the collagen comes from calf skin or rat tail tendon [31]. It is an easily obtainable abundant component of the ECM but must be used in a solubilized gel form for the preparation of HSEs, which has weak mechanical properties. This can be fixed via crosslinking or combining two or more natural polymers [41]. Aside from ECM components, to reconstruct the dermis, de-cellularized and synthetic polymers can also be employed [35].

To prepare a functional dermal equivalent, the 3D matrix must contain viable dermal fibroblasts. They are deposited on the dermal matrix. Here, they stop dividing and become synthetically active instead. During their cultivation, they reorganize the matrix by secreting components of the ECM. The fibroblasts contract, which allows for the next step in the preparation of HSEs [4; 31]. Epidermal keratinocytes are subsequently seeded onto the surface of the dermal equivalent into a concave area which should form in the middle of the 3D matrix [42]. The cultures are cultivated in submerged conditions. A crucial step in preparing the HSE is exposing the epidermal cells to the air. After few days, the cell culture inserts are lifted to the ALI, which triggers keratinocyte differentiation [31; 41]. The air-lift method marks the start of the culture time of organotypic cocultures. During this process, the nourishment from the culture medium is provided only by diffusion from below the cell culture inserts, which have a porous membrane [31]. This process lasts about two weeks. At the end of the cultivation, a fully cornified and stratified epidermis-like structure has formed with a similar structure to the native skin [35]. **Figure 5** demonstrates the comparison of natural *in vivo* human skin and a 3D skin equivalent.

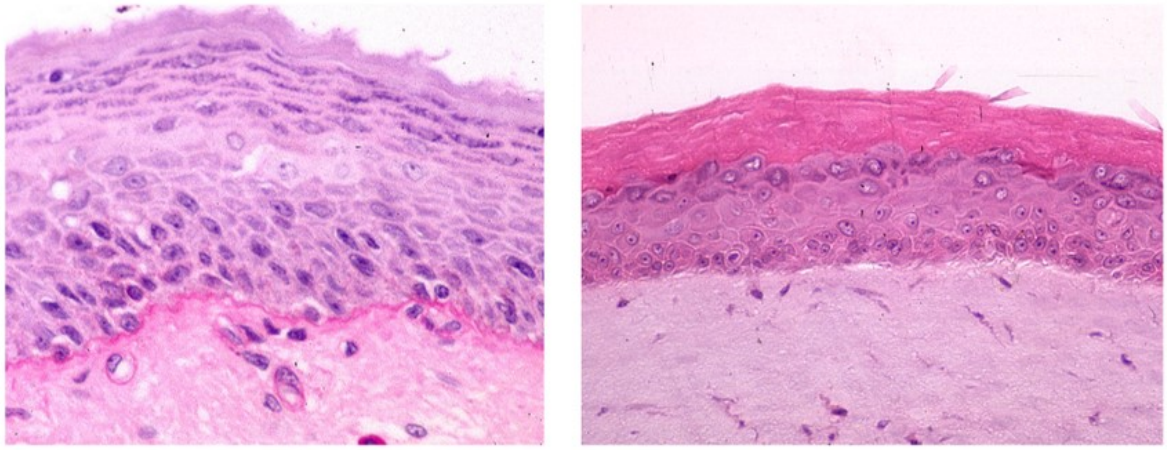

Figure 5: Histological cross section of human skin, and of the 3D skin equivalent with stratum corneum. Available from [43].

The resulting HSEs closely mimic the *in vivo* skin, however, they lack some elements of native skins' microarchitecture, such as vasculature and the presence of adipose tissue. This can be improved by equipping the HSE with appropriate cell types, however, such reality presents a limitation for the skin equivalents [41]. Vascularization is, for example, crucial to establish, as it allows the skin to maintain homeostasis and integration into the host tissue [29; 41]. Adipose tissue formation in HSEs would be beneficial for clinical practice and

research, as they would even closely mimic the native skin. So far, no skin equivalent with the subcutaneous layer is commercially available, however, attempts have been made to introduce cells isolated from adipose tissue obtained by liposuction into HSEs. So far, the results have proven to be very expensive cost-, material- and time-wise and advancements need to be made [41]. The physiological relevance of the skin equivalents could also be improved by introducing skin appendages, immune and nerve cells. While promising results have been produced, proper addition of other native skin elements is still in process [29; 35; 41]

Aside from the traditional protocol involving ALI cocultivation of OCSs, which can be lengthy, the development of 3D bioprinting techniques offers a potential solution to supply clinics and researchers alike with HSEs. This technique seems promising, as it allows for the reproduction of organs layer by layer and therefore could solve some shortcomings of traditionally prepared HSEs. This field, however, still requires more development in technology, availability, and price reduction [44].

II. ANALYSIS

4 MATERIALS AND METHODS

4.1 Biological material

NIH/3T3 is a fibroblast cell line isolated from a mouse (*Mus musculus*) NIH/Swiss embryo (ATCC – American Type Culture Collection), category number CRL-1658™). Grown routinely in T75 flasks (TPP, Trasadingen, Switzerland) in Dulbecco's Modified Essential Medium (DMEM) with 10% Calf serum (FCS; BioSera, France)) and 1% Penicillin/Streptomycin (GE Healthcare HyClone, United Kingdom) maintained at 37°C in humidified air and 5% CO_2. The cell culture medium was changed every second day. For routine passaging, NIH/3T3 cells were washed twice with Dulbecco's Phosphate Buffered Saline (PBS), trypsinized with Trypsin/EDTA (Biosera, France), and seeded at a 1:3 ratio. Cells were not allowed to reach >90% confluence.

Human Neonatal Dermal Fibroblast (HDF, Cat. N.: 106-05n, Cell Sigma-Aldrich) cell line originated from the human skin. It is responsible for the production of extracellular matrix in the skin. Cells were grown routinely in T75 flasks (TPP, Trasadingen, Switzerland) in Basal Medium Eagle (BME) with 10% fetal bovine serum (FBS, BioSera, France)) and 1% Penicillin/Streptomycin (GE Healthcare HyClone, United Kingdom) at 37°C in 5% CO_2. As with NIH/3T3 cell line, a routine passaging was chosen, including maintaining between 20-80% confluence and discarding if overconfluent.

In the case of Human Neonatal Epidermal Keratinocytes (HEK, Cat. N.: 102-05a, Cell Sigma-Aldrich), the cell line originated from the epidermis – the outermost layer of the skin. They produce keratin that helps maintain the barrier function of the skin. HEK cell line was maintained in the Keratinocyte Growth Medium 2 (KGM2, PromoCell, Germany) supplemented with the Keratinocyte Growth Medium 2 SupplementPack (PromoCell, Germany) and 1% Penicillin/Streptomycin (GE Healthcare HyClone, United Kingdom) at 37 °C in a humidified 5% CO_2 atmosphere. They were cultured until 90% confluence was reached and for routine passaging, cells were washed twice with PBS, trypsinized with Trypsin/EDTA and split at a 1:3 ratio into new flasks following standard cell culture methods. HEK was used in passages 6–8 in the experiment and the culture medium was changed every two days.

4.2 Prepared solutions

0.01M Acetic acid and 0.02M Acetic acid were prepared from a stock solution of 1M Acetic acid by diluting it with an appropriate amount of ultra-pure water (UPW).

4.3 Laboratory equipment and chemicals

Chemicals

Adenine (Cat. N.: 73-24-5; Sigma Aldrich, USA)

Amphotericin B 100X (Cat. N.: LM-A4109/100; Biosera, France)

Basal Medium Eagle (BME) powder (Cat. N.: B9638; Sigma-Aldrich, USA)

Calf Serum (FCS; Cat. N.: CA-115/500; Biosera, France)

Bovine collagen type I (Collado spol. s r. o., Czech Republic)

Type I collagen solution from rat tail (Cat. N.: C3867-1VL; Sigma Aldrich, USA)

Rat Tail Collagen Coating Solution (Cat. N.: 122-20; Sigma Aldrich, USA)

Collagen type I, High Concentration, Rat Tail (Cat. N.: 354249; Corning, USA)

Dulbecco's Modified Eagle's Media (DMEM) powder (Cat. N.: D5648; Sigma-Aldrich, USA)

Dulbecco's Phosphate Buffered Saline (PBS; Cat. N.: LM–S2041/500; BioSera, France)

Fetal Bovine Serum (FBS; Cat. N.: FB-1280; Biosera, France)

Gentamicin Sulfate (Cat. N.: LM-A4112/100, Biosera, France)

Ham's F12 – F12 Nut Mix (Cat. N.:2170-018; Life Technologies Limited, UK)

HEPES (Cat. N.: H0887-100ML; Sigma-Aldrich, USA)

Hydrocortisone (Cat. N.: 50-23-7; Sigma Aldrich, USA)

Insulin-Transferin-Selenium (ITS; Cat. N.: 414000-045; Life Technologies Corporation, USA)

L-glutamine 100X (Cat. N.: XC-T1715/100; Biosera, France)

$NaHCO_3$ (Cat. N.: 28000-31000; Penta Chemicals, Czech Republic)

NaOH (Cat. N.: 28000-31000; Penta Chemicals, Czech Republic)

O-phosphorylethanolamine (OEP; Cat. N.: 1071-23-4; Sigma-Aldrich, USA)

Penicillin-Streptomycin Solution 100X (Cat. N.: XC-A4122/100; Biosera, France)

Progesterone (Cat. N.: 57-83-0; Sigma Aldrich, USA)

Trypsin/EDTA 10X (Cat. N.: XC-T1717/100; Biosera, France)

3,3',5-triiodo-L-thyronine (T3; Cat. N.: 6893-02-3; Sigma-Aldrich, USA)

Laboratory machines and devices

Syringe filters 0,22 μm (Cat. N.: 99722, TPP – Trasandiger, Switzerland)

Incubator with accessories Heracell™ 150i (Thermo Scientific, USA)

Ultrasound Elmasonic S 70 H with heating (Elma, Germany)

Magnetic stirrer Arex digital (VELP Scientifica Srl, Italy)

Laminar flow hood Bio130 A2 with accessories (Alpina, Poland)

Extractor hood MERCI G NextGen (MERCI s. r. o., Czech Republic)

Centrifuge 5702 R cooled model for temperature-dependent samples (Eppendorf, Czech Republic)

Inverted microscope IX51 (Olympus, Japan)

Fluorescent microscope Olympus IX81 with phase contrast (OLYMPUS)

4.4 Used experimental and evaluation methods

4.4.1 Growth curve

The growth curve shows the change in the number of cells over time. It is an analytical instrument that allows for the growth characteristic study of a cell line, such as population doubling time (PDT). PDT can be used to quantify the cell reaction to inhibitory or stimulatory effects of a biological material or compound on cells and it also marks the right time to measure such effects. A typical cell growth curve consists of four phases: 1) lag-phase; 2) log-phase or exponential phase; 3) stationary phase; 4) death phase [45].

Cells after reseeding immediately enter the lag-phase, during which they recover from trypsinization. A cell during this phase does not divide, it focuses on spreading along the substrate, rebuilding its cytoskeleton, and the secretion of an extracellular matrix. It is a three-dimensional network composed of macromolecules, such as collagens, proteoglycans, laminins, fibronectin, elastin, and other glycoproteins [46]. Such structure facilitates adhesion between individual cells and their propagation along the substrate. These activities altogether allow cells to re-enter the cell cycle. A lag-phase can last from a few hours up to 48 hours [47].

Subsequently, a cell enters the log-phase, in which a cell population begins to grow exponentially by doubling at a characteristic rate. Such a phase can last up to 48 hours, varying on the type of cell line. After this exponential growth, when the nutrients from the substrate are all metabolized and the cells have occupied all of it, the cell population reaches

its maximum density and individual cells withdraw from the cycle as the population enters the stationary phase. During this phase, the growth rate drops to near zero, and the total number of cells does not change [47]. As the medium is all depleted, the number of dead cells surpasses the number of living cells.

To construct a growth curve, it is needed to work with a cell suspension of known cell concentration. The cells were passaged and at the end of this process, 1 ml of primary cell solution was acquired. To determine cell concentration in 1 ml of this solution, a 1:10 diluted cell suspension was prepared. From such liquid, a volume of 10 µl was pipetted onto a Bürker counting chamber and placed under an inverted microscope with 40x magnification. Cells were counted in a total of 40 squares. With the following **Equation (1)**, cell concentration in 1 ml of primary cell suspension was determined:

$$x = \frac{a \cdot 10^4}{n} \cdot z \tag{1}$$

Where x is the cell concentration, a is the number of cells, n is the number of squares and z is used dilution.

The resulting cell suspension had a concentration of 2×10^4 cells $\cdot$ ml^{-1} in the total culture media volume. Next, 3 ml of cell suspension was transferred into each 35mm petri dish using a 10 ml automatic pipette. Testing was done in duplicate for each day. Cell culture dishes were placed into an incubator for 24 hours. The temperature inside the incubator was 37 °C and the concentration of CO_2 was 5 %.

After the first 24 hours, a set of two cell culture dishes were taken from the incubator and passaged. The counting of cells was done in the same manner as previously. This process was repeated in regular intervals of 24 hours for 10 days, with a change of culture media every 72 hours.

From the obtained values of cell numbers, PDT can be calculated using the following **Equation (2)**:

$$PDT = \frac{\Delta t}{log_2\left(\frac{\Delta N}{N_0 + 1}\right)} \tag{2}$$

Where Δt is the difference between the time at the start and the time when cell concentration was the highest, ΔN is the change of cell concentration during the cultivation time and N_0 is the initial concentration of cells.

4.4.2 *In vitro* scratch assay

Scratch assay, also called wound healing assay, performed *in vitro* is a method used for the assessment of cell migration in a controlled experimental environment of a confluent monolayer [48]. Cell migration is the ability of a cell or a cell sheet to move in a certain direction from one location to another as a response to chemical and mechanical signals [49]. It plays a crucial role in wound healing, as cells need to migrate as well as proliferate in a wound bed to facilitate re-epithelization of the skin tissue [50].

Scratch assay is a cost-effective method suitable for adherent cell lines, such as fibroblasts and epithelial or endothelial cells. Aside from its inexpensive character and simplicity, another major benefit is that scratch assay, to some extent, mimics cell migration *in vivo* [51]. By changing experimental conditions and introducing a possible stimulatory or inhibitory compound, we can observe its effects on the subculture to evaluate how cells react to new conditions [50]. Aside from studying possible therapeutic compounds before clinical use, we can also study how substrate-coating materials, such as collagen, affect cell behavior [52].

Scratch assay protocol is based on observing cell migration into a cell-free space carved in a confluent monolayer by a sharp object, such as a pipette tip. A chosen space is then monitored under a microscope and captured into images via a camera [52]. There are many methods to quantify the measured data, with the most common one focused on calculating wound healing rate by determining wound width and wound area. This method is inexpensive, but can be time-consuming, as it requires manually measuring the area and width at different time points and then calculating the difference between them. Other more advanced methods are also available that incorporate a real-time automated optical camera that uses built-in software, which can track cells and determine proliferation and migration [48; 50].

1) Preparation of bovine collagen type I solutions

For the *in vitro* scratch assay, different concentrations of Collagen A (Bovine collagen type I; Collado spol. s r. o., Czech Republic) were prepared in two sets by dissolving them in

particular solvents. The first set was prepared by dissolving the collagen in 0.01M acetic acid, and the second set was prepared by dissolving collagen in UPW. The individual collagen concentrations are shown in **Table 2**.

Table 2: Preparation of collagen solutions

Collagen concentration [mg/ml]	Collagen concentration [%]	Collagen load [mg]
1	0.1	20
2	0.2	40
4	0.4	80
12	1.2	240

An appropriate load of bovine collagen type I was weighted on analytical scales with an accuracy of 0.0001 g. To dissolve the collagen, 20 ml of solvent was added into a beaker with the collagen. The dissolving process consisted of first letting it swell for 3 hours and then stirring it for 24 hours at 30 °C on a magnetic stirrer.

2) *In vitro* scratch assay

To coat the cell culture plates, Collagen A solutions in 0.01M acetic acid were used, along with two additional collagens: Collagen B (Collagen type I solution from rat tail; Sigma Aldrich, USA) and Collagen C (Rat Tail Collagen Coating Solution; Sigma Aldrich, USA). Additionally, 0.4% Collagen I solution was used to prepare a Collagen A solution with the protein concentration of 0.048 $\mu g \cdot \mu l^{-1}$, which will further be referenced as Diluted Collagen A. This solution was prepared utilizing the **Equation (3)** below. Layer density (collagen $\cdot$ cm^{-2}) was translated to collagen concentration (collagen $\cdot$ ml^{-1}). For coating, the desired layer density of collagen was 5-10 $\mu g \cdot cm^{-2}$.

$$c = \frac{A \cdot x}{V} \tag{3}$$

Where c is the collagen concentration, A is the surface area of the well in the cell culture plate, x is the layer density of collagen and V is the pipetted volume of the collagen solution.

Table 3 below shows collagen solutions and the volume that was used for coating the wells of cell culture plates.

Table 3: Collagen solutions and volume used for coating

Collagen solution	V [µl]
0.1% Collagen A	1,000
0.2% Collagen A	1,000
0.4% Collagen A	1,000
1.2% Collagen A	1,000
Diluted Collagen A	1,000
Collagen B	1,000
Collagen C	700

After coating the surface of the wells in the collagen solutions, cell culture plates were incubated at 37 °C for 30 minutes. To seed the cells into the cell culture plates, they were firstly passaged and then cell concentration was determined by counting the cells using a Bürker chamber. Cell suspension obtained by cell passaging was diluted with culture media, so that the final cell concentration was 300 000 cells per well. After the seeding, the culture plates were incubated at 37 °C for 24 hours. The next day, a scratch in the confluent cell monolayer was created by carving a vertical line in the middle with a 1ml pipette tip. This scratch was monitored immediately after it was created, then subsequently after 4, 6, and 24 hours.

To quantify how much the wound closed, two evaluation methods were used. First was calculating the wound closure area, which is expressed by the **Equation (4)**. Here, the initial and final values of the wound area were compared. Using this evaluation method, the rate of migration is expressed as a percentage reduction of area in the cell-free space.

$$Wound\ closure = \frac{A_i - A_f}{A_i} \cdot 100\ \% \tag{2}$$

Where A_i is the initial area of the wound and A_f is the final area of the wound.

The second method is expressed by the **Equation (5)**. The average diameter between the edges of the wound determines the wound width. Under normal conditions, it decreases with time as the cells migrate, therefore the quantification using this evaluation method is based on comparing initial and final width in time.

$$R_m = \frac{W_i - W_f}{t} \tag{3}$$

Where R_m describes the rate of cell migration, W_i is the initial width of the wound, W_f is the final width of the wound and t is the duration of migration.

4.4.3 Preparation of organotypic skin model

1) Preparation of acellular layer

The acellular layer is prepared by polymerizing collagen, which forms a hydrogel. Prior to the polymerization, the acidic solution of collagen needs to be neutralized, so that its final pH is around the value of 7,4. The reason for such an adjustment is because the physical properties of the collagen hydrogel are very dependent on the pH during polymerization.

A neutralization buffer was prepared to neutralize the acidic collagen solution. The reagents used in this mixture are shown in **Table 4** along with their respective volumes. These volumes correspond to a collagen concentration of 4 mg · ml^{-1} that was dissolved in 0.02M acetic acid. The used collagen was Collagen D (Collagen type I, High concentration, Rat Tail; Corning, USA). Such prepared buffer was sterile-filtered and stored in a fridge until use.

Table 4: Preparation of neutralization buffer

Components	V [ml]
10× PBS	10.000
HEPES	2.000
7.5% $NaHCO_3$	6.000
1M NaOH	0.575
UPW	56.400
Final volume	74.975

The final neutralized collagen was prepared at a concentration of 1 mg · ml^{-1} by pipetting 750 µl of neutralization buffer into an Eppendorf tube and adding 250 µl of Collagen D solution with protein concentration of 4 mg · ml^{-1} into it. The content of the tube was homogenized by slow, repeated pipetting, to avoid bubble formation. The mixture was centrifuged at 4 °C at 4,400 RPM for one minute to remove any accidental bubbles. Working

in low temperatures was crucial to prevent the protein from premature polymerization, therefore the preparation of neutralized collagen was performed on ice.

Next, 250 µl of the neutralized collagen mixture was pipetted into the wells of a 12-well plate cell culture inserts and incubated at 37 °C for one hour. During this time, the collagen polymerized and generated a clear hydrogel. Then, 1 ml of PBS was added on top of the hydrogel and stored in the incubator until use few hours later. Before use, PBS was aspirated.

2) Preparation of cellular layer

To supply the cells seeded into the collagen lattice, cast feed medium was prepared by mixing the ingredients in **Table 5** together. Such solution was then sterile-filtered and used for a maximum of seven days.

Table 5: Preparation of cast feed medium

Components	V [ml]
5× BME	10.00
L-glutamine	1.00
FBS	5.00
Gentamicin	0.05
7.5% $NaHCO_3$	1.30
UPW	34.00
Final volume	51.35

For the same reason as before, all parts of this step mentioned below were done on ice to maintain a low temperature. First, a pre-mix solution was prepared according to **Table 6**. After mixing all the ingredients, the solution was sterile-filtered.

Table 6: Preparation of pre-mix solution

Components	V per well [µl]
5× BME	395
L-glutamine	39
Gentamicin	5
7.5% $NaHCO_3$	120
FBS	440
Final volume	999

When the pre-mix solution was prepared, the culture HDF was trypsinized and pelleted in a falcon tube by centrifuging at 1,400 RPM for 3 minutes. The supernatant was aspirated and 1 ml of BME was added into the tube. Cells were counted using a Bürker counting chamber.

In a 15ml falcon tube, neutralized collagen was combined with premix solution and mixed well. The HDF cells were added to such prepared collagen mixture and swirled while avoiding bubble formation. The used volumes of these three components are written down in **Table 7** below. Subsequently, 720 µl of this mixture was pipetted into each insert on top of the acellular layer. The 12-well plate with this gel was put into an incubator at 37 °C for 2 hours to ensure the gel's polymerization. After the 2-hour mark, 1.2 ml of cast feed medium was added to the bottom wells. The medium was changed the next day and refilled with fresh cast feed medium now in the bottom and the top wells. For the next 7 days, the plates were left in the incubator with the change of medium every 2-3 days.

Table 7: Preparation of cellular layer

Components	V per well [µl]
Pre-mix solution	153.00
HDF cell suspension	81.75
Neutralized collagen	500.00

3) Seeding of keratinocytes on collagen lattice

Epidermalization medium was prepared and sterile-filtered right after mixing the ingredients. The medium consists of ingredients listed below in **Table 8**.

Table 8: Preparation of epidermalization medium

Components	V [ml]
5× BME	15.00
5x Ham's F12	5.00
L-glutamine	2.00
7.5% $NaHCO_3$	1.95
FCS	0.30
ITS	0.20
Adenine	0.20
T3	0.20
Progesterone	0.20
OEP	0.20
Amphotericin B	0.10
Gentamicin	0.10
Hydrocortisone	0.08
UPW	76.00
Final volume	101.53

Afterward, a culture of HEK was trypsinized and pelleted in a falcon tube by centrifuging at 1,400 RPM for 3 minutes. The supernatant was aspirated, and the cells were resuspended in 1 ml of the epidermalization medium. Cells were counted using a Bürker counting chamber.

The cast feed medium was aspirated from both the top and bottom wells. Next, 30 µl of the HEK cell suspension was added into the center of the inserts with polymerized gel with HDF and left in the laminar flow hood for 5 minutes, so that the medium soaks into the gel. For the cells to attach, the 12-well plate was transferred into the incubator at 37 °C for 2 hours. After the two-hour mark, epidermalization medium was added into each bottom well in the volume of 750 µl and into each top well in the volume of 300 µl. For the next 7 days, the plates were left in the incubator with the change of medium every 2-3 days.

4) Differentiation of the epidermal layer at the ALI

Cornification medium was prepared and sterile-filtered right after mixing the ingredients. The medium consists of ingredients listed below in **Table 9**.

Table 9: Preparation of cornification medium

Components	V [ml]
5× BME	10.00
5x Ham's F12	10.00
L-glutamine	2.00
FCS	2.00
7.5% $NaHCO_3$	1.30
ITS	0.20
Adenine	0.20
T3	0.20
OEP	0.20
Amphotericin B	0.10
Gentamicin	0.10
Hydrocortisone	0.08
UPW	76.00
Final volume	102.38

After the cornification medium was prepared, the epidermalization medium was aspirated from both the top and bottom wells. The inserts with gel were removed from the 12-well plate and moved to a temporary plate. Sterile cotton pads were added with forceps into the bottom wells of the 12-well plate, ensuring the inserts would be exposed to the air. These cotton pads were then soaked in 720 µl of epidermalization medium and would allow the inserts to be fed with medium only from below. The inserts were transferred back to the original 12-well plate while avoiding air bubble formation. The medium in the bottom well was ensured to be slightly above the level of the membrane of the insert. The plate was transferred into the incubator at 37 °C and maintained for 7 days, with change of medium every 2-3 days.

5) ALI cultivation

The maintenance medium was prepared and sterile-filtered right after mixing the ingredients. The medium consists of ingredients listed below in **Table 10**.

Table 10: Preparation of maintenance medium

Components	V [ml]
5× BME	10.00
5x Ham's F12	10.00
L-glutamine	2.00
FCS	2.00
7.5% $NaHCO_3$	1.30
ITS	0.20
Adenine	0.20
T3	0.20
OEP	0.20
Amphotericin B	0.10
Gentamicin	0.10
Hydrocortisone	0.08
UPW	76.00
Final volume	102.38

The cornification medium was aspirated, and 720 µl of maintenance medium was added into each bottom well. The plate was transferred into the incubator at 37 °C for the next 7 days, with the change of medium every 2-3 days. Two weeks after the transition to an ALI interface, the skin cultures are ready to be harvested for histological analysis.

5 RESULTS

5.1 Construction and analysis of growth curve

For the construction of the growth curve, two sets of cells were collected for each day. Values of cell numbers for the same day were averaged and cell concentration calculated for every 24 hours of the experiment. The result can be seen in **Table 11**.

Table 11: Average number of cells per day and cell concentration

Time [h]	Cell number	Cell concentration [10^7]
24	89.5	22.375
48	203.0	50.750
72	434.0	108.500
96	535.5	133.875
120	406.5	101.620
144	143.0	35.750
168	168.5	42.125
192	177.0	44.250
216	131.0	32.750
240	132.5	33.125

Using the data from **Table 11**, the dependence of cell concentration on cultivation time was constructed and can be seen in **Graph 1**. Furthermore, using **Equation (2),** PDT for the NIH/3T3 cell subculture was established to be 41.72 hours.

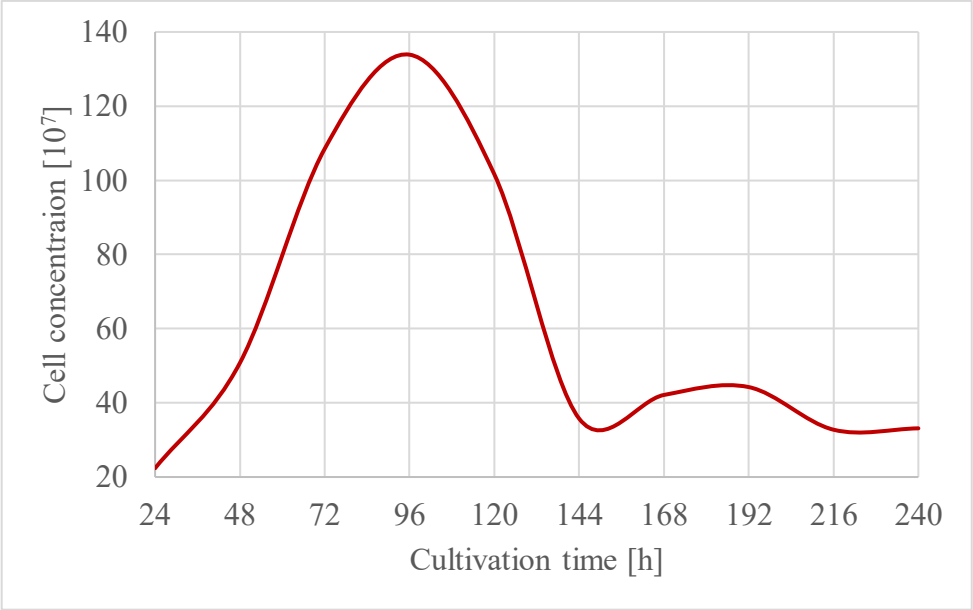

Graph 1: Dependence of cell concentration on cultivation time.

5.2 Evaluation of *in vitro* scratch assay

1) Preparation of bovine collagen type I solutions

After 24 hours, the solutions were transferred from the beakers into plastic tubes and stored in the fridge until use. Resulting Collagen A solution was a gel-like liquid with thickness increasing as the protein concentration increased, along with the color changing from translucent to opaque, which can be seen in **Figure 6** and **Figure 7**.

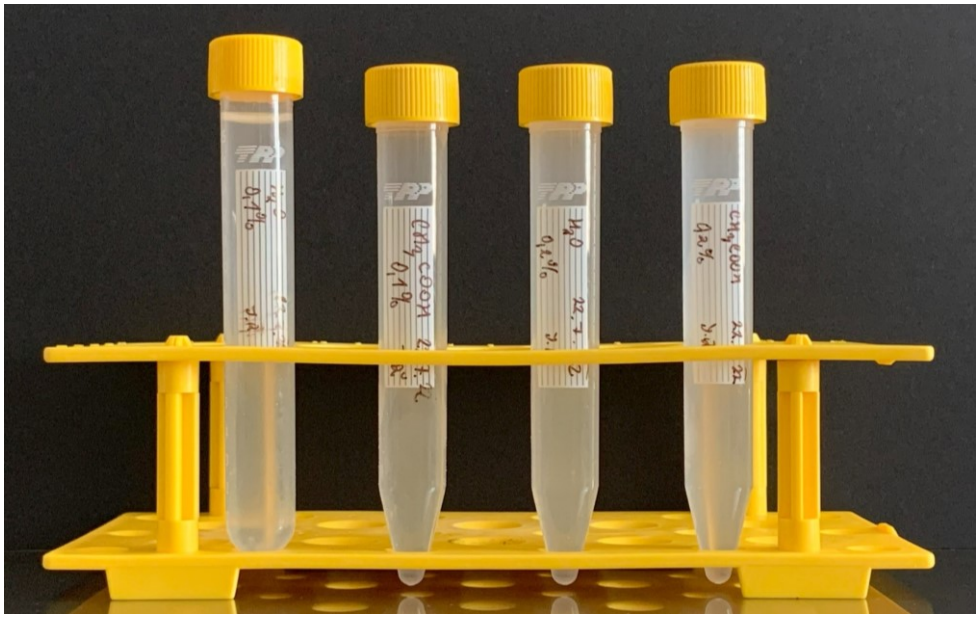

Figure 6: Prepared Collagen A solutions. From the left: 0.1% Collagen A in UPW, 0.1% Collagen A in 0.01M acetic acid, 0.2% Collagen A in UPW, 0.2% Collagen A in 0.01M acetic acid.

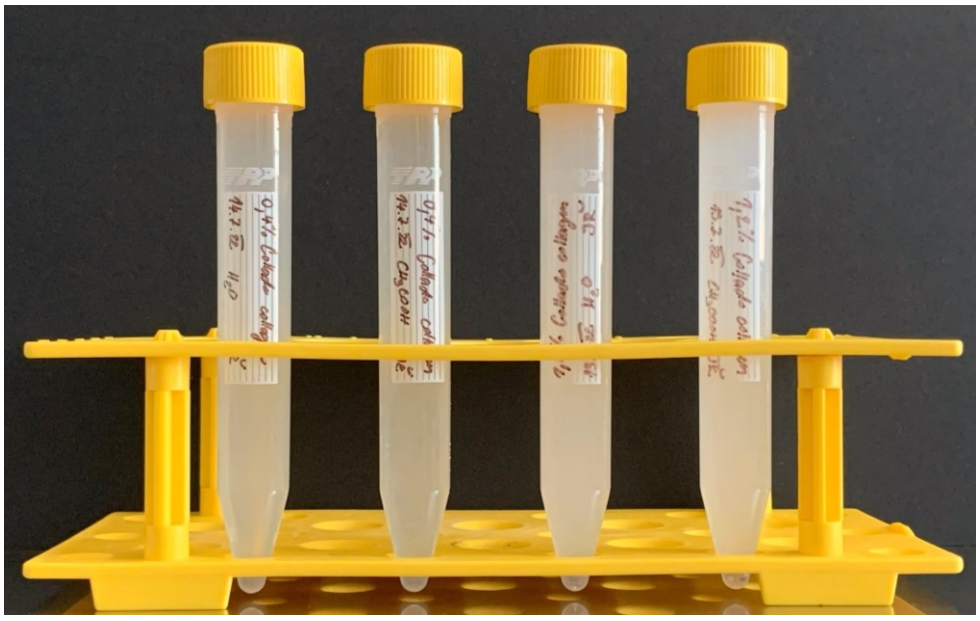

Figure 7: Prepared Collagen A solutions. From the left: 0.4% Collagen A in UPW, 0.4% Collagen A in 0.01M acetic acid, 1.2% Collagen A in UPW, 1.2% Collagen A in 0.01M acetic acid.

2) *In vitro* scratch assay

The wound was monitored immediately after its creation, then after 4, 6, and 24 hours with a fluorescent microscope with phase contrast. Images of the wound were captured by the in-built camera of the microscope. The area and the width of the cell-free space were measured

using the software functions of the camera. **Table 12** shows the area measurements of selected samples. The values of the wound area were used to calculate how much the wound closed in % by utilizing **Equation (4)**. The calculated values are shown in **Table 13**.

Table 12: Area of the wound in mm^2

Time [h]	Positive control	Reference	Diluted Collagen A	Collagen B
0	1.006	0.979	0.811	1.082
4	0.898	0.993	0.702	1.104
6	0.915	0.999	0.629	0.983
24	0.812	0.000	0.000	0.044

Table 13: Wound closure area in %

Time [h]	Positive control	Reference	Diluted collagen A	Collagen B
24	19.32	100.00	100.00	95.91

Along with the area of the cell-free space, its width was also measured. Its values for certain samples are shown in **Table 14**. Using this data, rate of migration was calculated using **Equation (5)** and the values can be found in **Table 15**.

Table 14: Width of the wound in mm

Time [h]	Positive control	Reference	Diluted collagen A	Collagen B
0	0.893	0.583	0.439	0.608
4	0.521	0.641	0.404	0.626
6	0.533	0.581	0.362	0.555
24	0.520	0.000	0.000	0.148

Table 15: Rate of migration in $mm \cdot h^{-1}$

Time [h]	Positive control	Reference	Diluted collagen A	Collagen B
24	0.016	0.024	0.018	0.019

The efficacy of each collagen sample and its concentrations were evaluated by comparing them to the reference sample. All collagen A concentrations, except for the concentration of 1.2%, had a positive effect on cell migration. Collagen B and C samples showed worse performance at benefiting cell migration and for further use would require to be diluted.

Figure 8 below shows the wound closure process of the sample of diluted Collagen A over time. The first photograph in the top left shows how this sample looked immediately after creating the wound. In the top right, the sample was photographed at the 4-hour mark. Here, several migrating cells can be seen at the edges of the wound. The same applies to the sample at the 6-hour mark in the bottom left, where the migrating cells are a little bit more noticeable. In the bottom right, the sample is at the 24-hour mark and the cells have nearly filled the cell-free gap. When compared to the reference sample which is shown in **Figure 9**, some differences can be observed in the density of migrated cells after 24 hours. **Figure 10** furthermore shows differences between selected samples after 24 hours after creating the scratch.

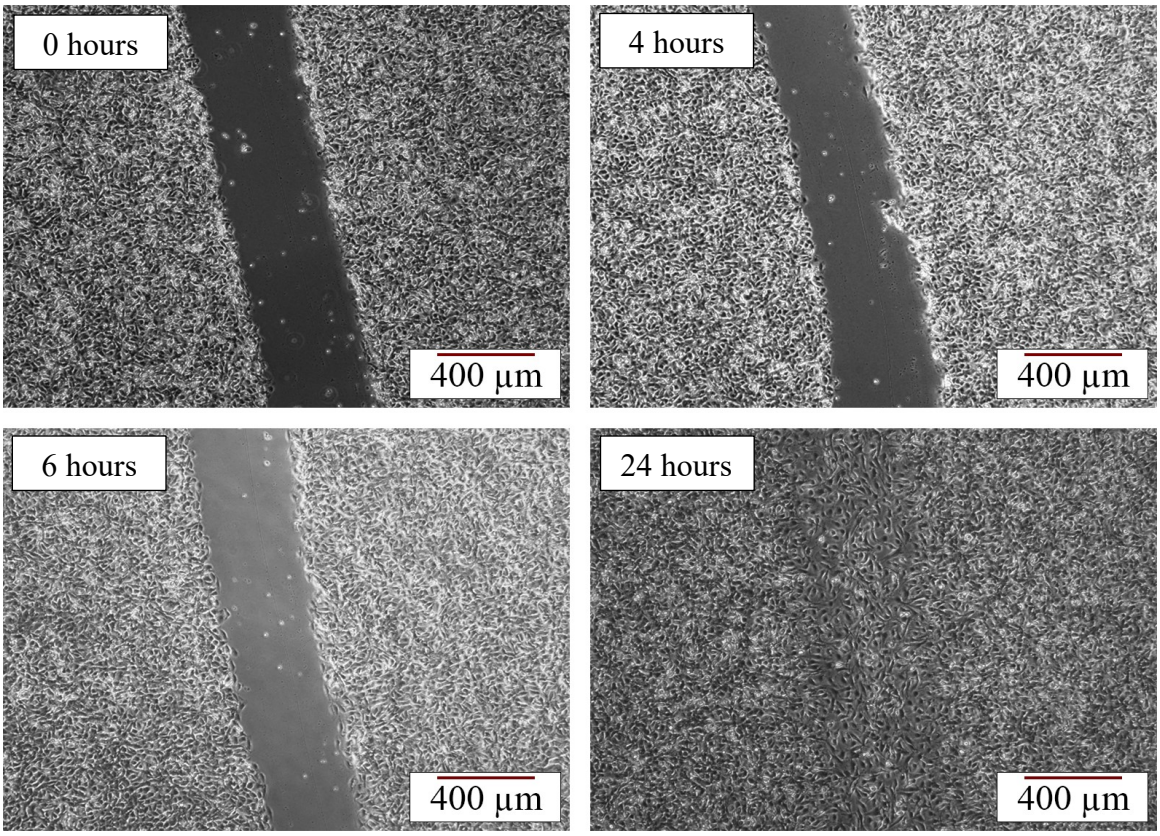

Figure 8: Sample of Diluted Collagen A over 24 hours, magnified 40x.

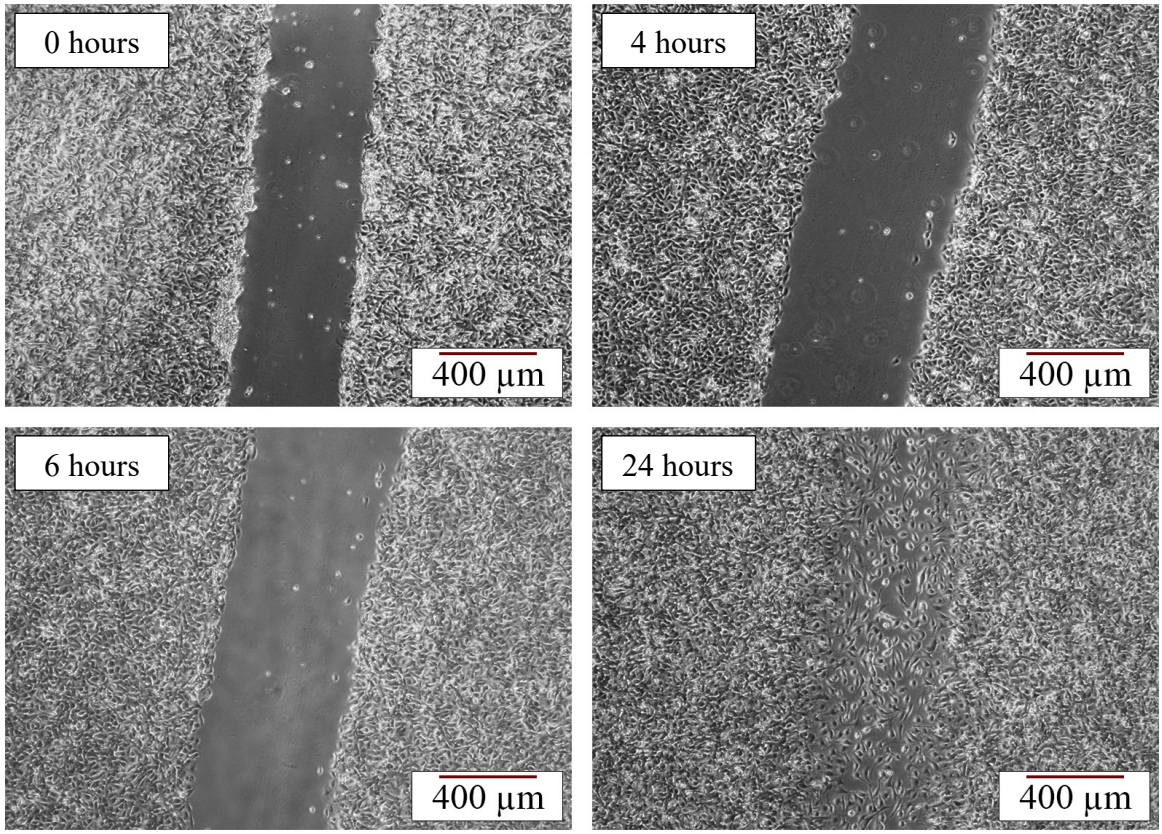

Figure 9: Reference sample over 24 hours magnified 40x.

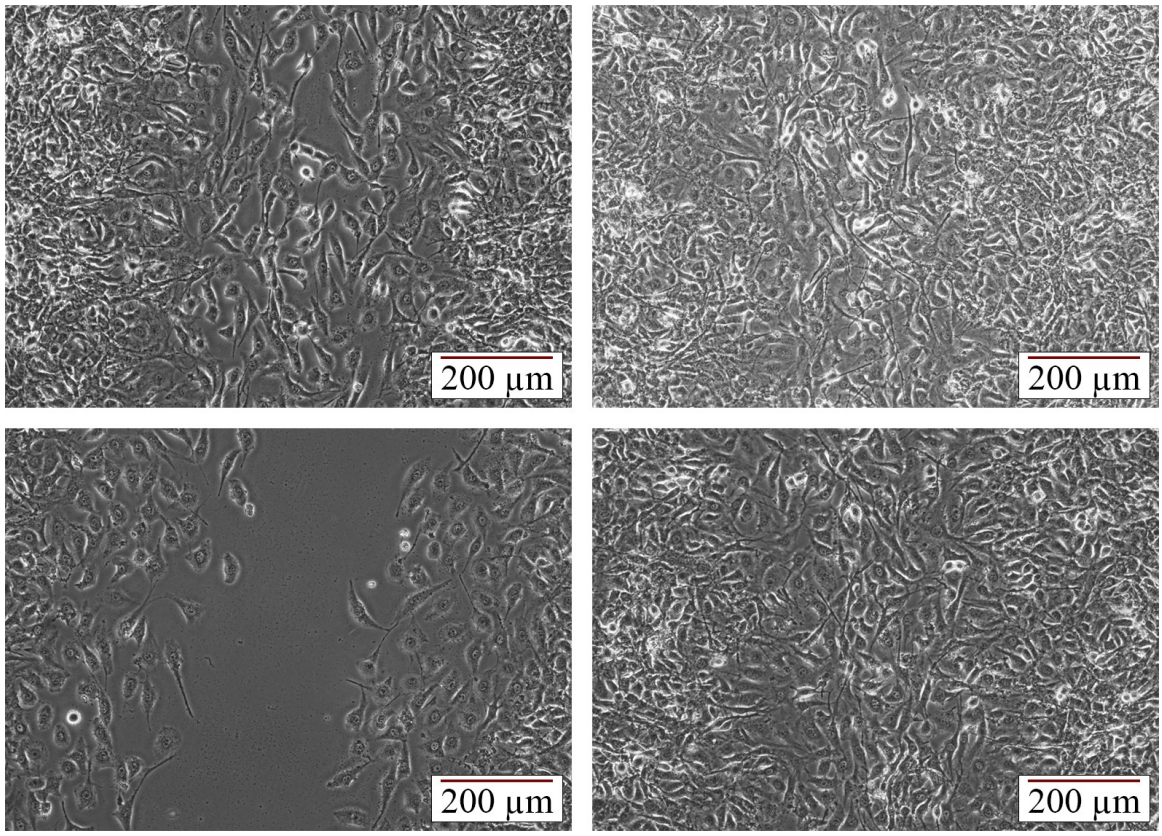

Figure 10: The scratch after 24 hours in various samples magnified 100x. Top left: reference, top right: 0.4% Collagen A, bottom left: Collagen B, bottom right: Diluted Collagen A.

5.3 Organotypic skin model

1) Preparation of acellular layer

Due to problems with the polymerization of Collagen A solutions, Collagen D was introduced and used to prepare the acellular layer. Firstly, the acidic solution of Collagen D was neutralized by the prepared neutralization buffer. Subsequently, the neutralized collagen was pipetted into cell culture inserts and incubated. The result was a thick gel formed by collagen polymerization, which will work as a scaffold for the HDF cells. As shown in **Figure 11**, the gel is translucent in color and does not flow.

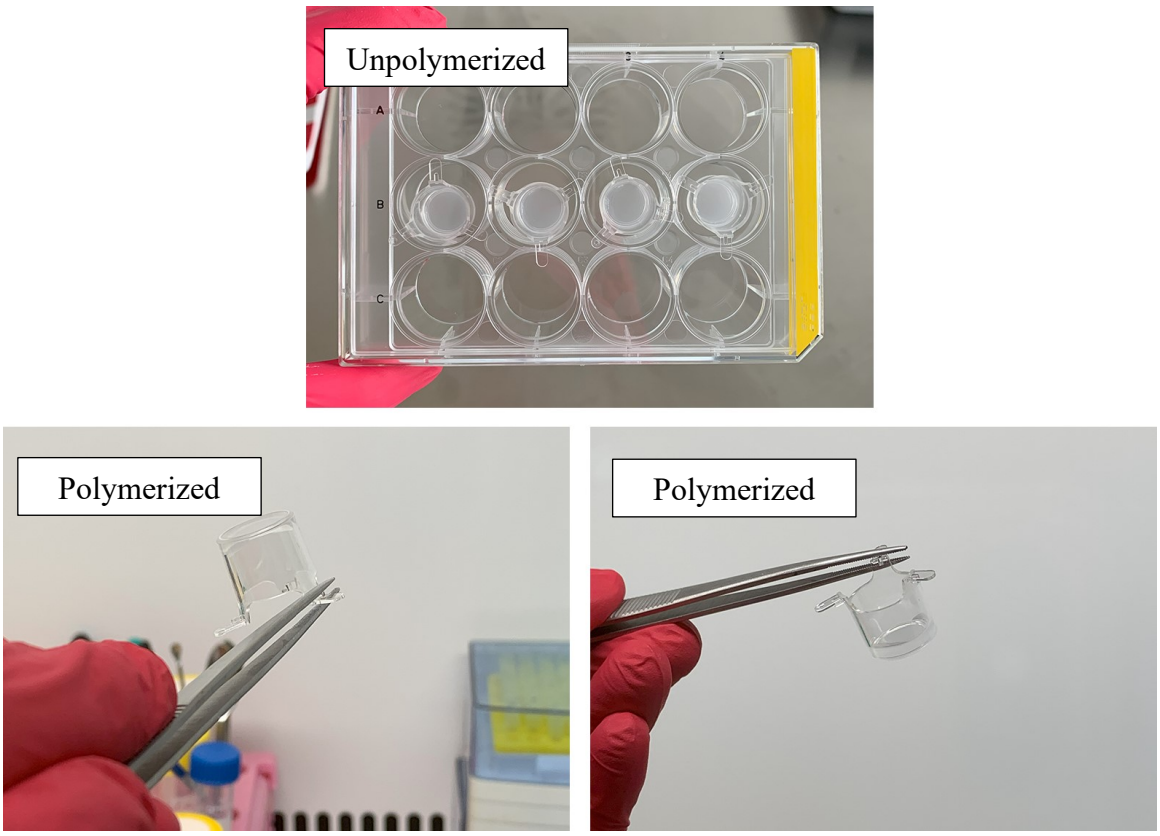

Figure 11: Preparation of acellular layer. Top: unpolymerized collagen gel before incubation. Bottom: Collagen gel after polymerization.

2) Preparation of cellular layer

After the acellular layer was prepared, the mixture of HDF cell culture and pre-mix solution was pipetted onto it and then put into the incubator to polymerize. Cast feed medium was added into bottom wells only to supply the cells inside the cell culture inserts from below. The cast feed medium was added to the top wells two days later during the medium replacement. As shown in **Figure 12**, the polymerized collagen gel seeded with the mixture

of HDF was translucent pink in color, which roughly corresponded to the color of the cast feed medium, and thick in substance.

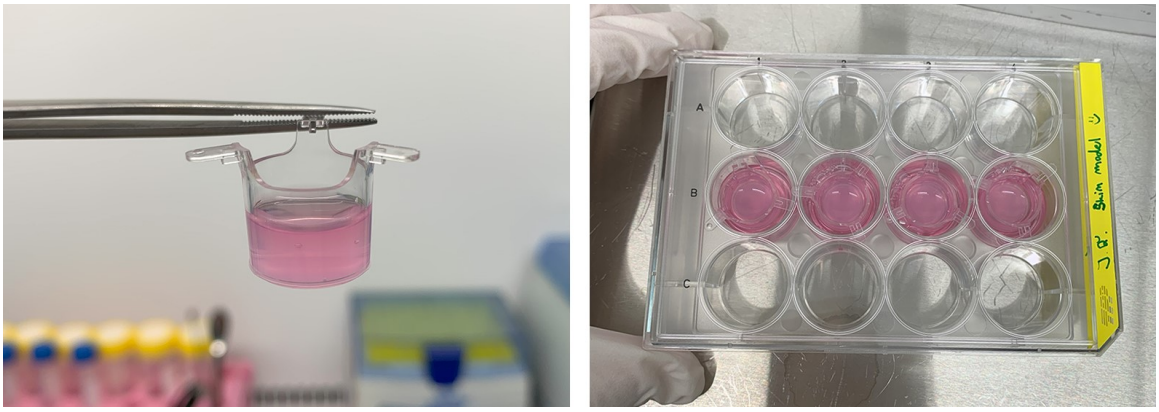

Figure 12: Preparation of cellular layer. Left: Cell culture inserts with polymerized collagen with the culture of HDF. Right: 12-well plate with cast feed medium only in the bottom wells.

3) Seeding of keratinocytes on collagen lattice

One week after seeding the HDF, the collagen lattice shrunk slightly and formed a concave area in the middle, where the HEK cells suspended in epidermalization prepared earlier were pipetted. This can be seen in **Figure 13** on the left photograph.

Figure 13: Seeding of keratinocytes on collagen lattice. Left: cell culture plates before seeding the HEK cells atop the dermal matrix. Right: Cell culture plate after seeding the HEK cells.

4) Differentiation of the epidermal layer at the ALI

To create a proper skin equivalent, differentiation of the epidermal layer will be induced by lifting the cell culture inserts to the ALI. The transition to such phase is crucial in creating a proper skin equivalent, as the keratinocytes are allowed to form a proper epidermal layer.

This step could not be completed due to the discovery of bacterial contamination, which can be seen in **Figure 14**. Visible colonies have been inspected under a microscope. Visually, singular cells resembled yeast cells in appearance, however, due to the microorganism being in the 3D structure of the matrix, it was hard to observe. For safety and prevention of further spread, all samples of the would-be skin equivalents were immediately discarded.

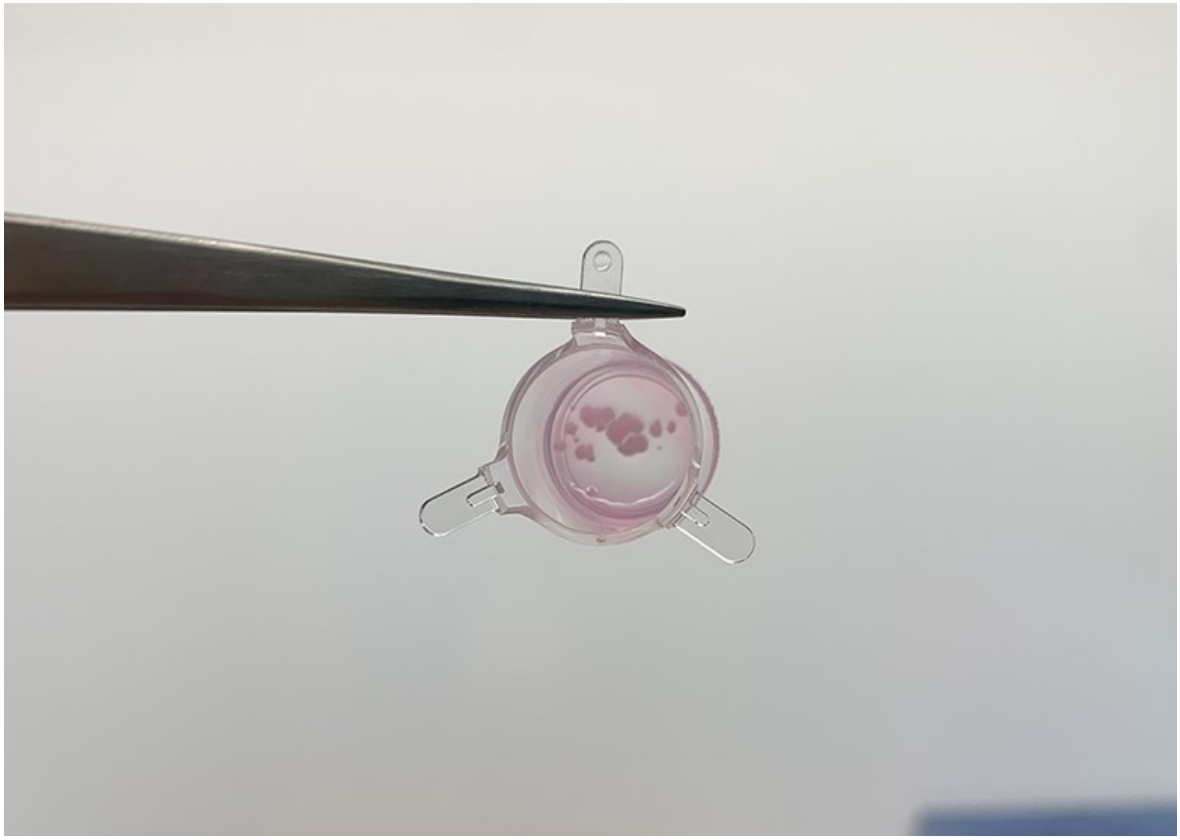

Figure 14: Discovery of microbial contamination the day the cell culture plates were to be lifted to the ALI.

6 DISCUSSION

For the construction of the growth curve, as it has been previously stated in **Chapter 4.4.1**, it typically consists of four phases: 1) lag-phase; 2) log-phase or exponential phase; 3) stationary phase; 4) death phase. The cells have managed to double in numbers in almost 42 hours since trypsinization, where they entered the exponential phase. The most significant growth happened roughly between hour 48 and hour 96, where the slope of the growth curve is high. The population appears to have entered the stationary phase somewhere around the 96th hour, after which it quickly began to decline. The growth curve as it was constructed had an expected course. Its progress corresponds to theoretical knowledge of cell line behavior in an *in vitro* culture.

The result of *in vitro* scratch assay corresponds with the theoretical knowledge of the effects of collagen on cell behavior. Surface coating with components of ECM, which collagen is a part of, plays a role in providing adhesive cell surface and participates in signaling that is involved in cell migration. Specifically, collagen binds to mediator proteins in the cell membrane and thereby mediates the cells signal transmission. Aside from cell migration, collagen may also affect cell proliferation, too, by this mechanism [20; 52]. For surface coating, literature and manufacturers recommend collagen type I coating concentration of around 1-10 $\mu g \cdot cm^{-2}$, which corresponds to 1-10 $\mu g \cdot ml^{-1}$ [53; 54; 55]. Such values correspond with the concentration used for coating in this experiment.

The bovine collagen type I prepared for the *in vitro* scratch assay was unfortunately not suitable for the preparation of the organotypic skin model due to its inability to polymerize in an incubator. Collagen from rat tail tendon had to be utilized and showed desirable results for the preparation of said skin model.

At the beginning of week 3 of the preparation bacterial contamination was discovered, and the model was discarded. Potential causes of bacterial contamination of cell cultures include the operator, the laboratory environment, other cells, and reagents. In most cases, contamination can be prevented by following good aseptic techniques and managed by immediately discarding affected cultures and reagents as soon as they are spotted. Other ways of managing contamination include the use of antibiotics. However, the contamination may persist despite antibiotic treatment and even re-emerge with increased resistance to the

employed antibiotic. Therefore, an emphasis is put on the fact that, in most cases, routine cell culture should be performed without the use of antibiotics [56].

Macroscopically visible changes should be visible after the cells are lifted and cultured at the ALI. Until then, no crucial change in the matrix should take place. After the airlift, the culture is exposed to air over the course few weeks and the epithelium consisting of HEK differentiates, forming a stratified and cornified epidermis at the end of the process [35; 42]. Additionally, the translucent color of the matrix should change during this process to an opaque color. When the cultures are exposed to air, the surface of the matrix should be covered in a granular disc, which consists of newly undifferentiated cells. As they differentiate, the disc should change its color to white and get larger until harvesting [42].

Such prepared skin model corresponds to traditional approaches to engineering a 3D skin equivalent that was established in the late 20^{th} century. These models of the skin are useful tools in the laboratory for studying skin structure and physiology. They can be further modified to correspond to certain pathological conditions, which can be studied to gain insight into a certain state. Nonetheless, they are not completely relevant to the native skin, as they are devoid of skin appendages, vasculature, innervation, and immune cells, and they do not display the dermal heterogeneity as the native skin. Additionally, they have a relatively short shelf life and the *in vitro* skin equivalents degenerate after just a few weeks [35; 41; 42].

CONCLUSION

The main aim of this bachelor's thesis, together with the literary review of human skin and tissue engineering of such organ, was the preparation of a 3D organotypic model of the human skin based on *in vitro* cocultivation of HEK with HDF on a collagen lattice.

In the theoretical part, it has been established that the structure of the human skin is complex and contributes to its many physiological functions. The damage to the skin has a negative effect on our health depending on the severity of the injury. Especially full-depth wounds impact the physiology of the damaged skin site due to scar formation. Some wounds can also become chronic, resulting in delayed healing. Thanks to recent advancements in TE, successful skin substitutes were developed and utilized in medical practice to promote the healing of skin injuries, especially acute burn wounds and chronic wounds. These advancements have led to the preparation of the first 3D HSE by coculturing dermal fibroblasts and epidermal keratinocytes on a collagen type I lattice. Since then, more types of skin equivalents have been established. Because these models share a similar structure to human skin, their use has been widely beneficial in basic research, drug formulation, and in the clinic. Despite new advancements, these models remain relatively costly when compared to different skin tissue engineering approaches. Another shortcoming of HSEs is the absence of certain components present in the native skin, such as vasculature and adipose tissue, to name a few. Incorporating native elements of the skin into the HSE structure would greatly improve their performance, however, certain developments still need to be made in this regard.

In the practical part of this thesis, a fibroblast cell line of NIH/3T3 cells was characterized by constructing its growth curve. Additionally, the data from the growth curve were utilized to establish PDT for this cell line. The result is 41.72 hours. Further, the behavior of NIH/3T3 cells in response to various concentrations of collagen type I was studied with an *in vitro* scratch assay. The objective of this method was to confirm which collagen type I concentrations were suitable for cell cultivation according to the recommended values. The results were then used for the preparation of the organotypic skin model, which employs an acellular layer made of collagen type I. For the construction of the growth curve and *in vitro* scratch assay, NIH/3T3 fibroblast cell line has been used thanks to their accessibility and easy maintenance in culture. The cell lines employed for the preparation of the 3D organotypic skin model were organotypic cultures HDF and HEK. They represent the main type of cells found in the human dermis and epidermis respectively. Due to bacterial

contamination, the skin model was discarded. It could not be prepared anew with new biological material with the reason being lack of time to thaw new cells, culture them to the desired confluency and coculture them together to prepare a new skin model. The cause of contamination has not been investigated.

BIBLIOGRAPHY

[1] *Exclusive: Whatever Happened to the Mouse with the Ear on Its Back?* [online]. 2017 [cit. 2023-05-17]. Available from: https://www.newsweek.com/tissue-surgeon-ear-mouse-human-organs-transplant-cell-phones-666082

[2] CAO, Yilin, Joseph P. VACANTI, Keith T. PAIGE, Joseph UPTON a Charles A. VACANTI. *Transplantation of Chondrocytes Utilizing a Polymer-Cell Construct to Produce Tissue-Engineered Cartilage in the Shape of a Human Ear* [online]. 1997, **100**(2), 297-302 [cit. 2023-05-17]. ISSN 0032-1052. Available from: doi:10.1097/00006534-199708000-00001

[3] *Mouse with human ear* [online]. 2006 [cit. 2023-05-17]. Available from: https://www.abc.net.au/science/articles/2006/06/02/1644154.htm

[4] BOER, Jan de a Clemens VAN BLITTERSWIJK, ed. *Tissue engineering*. 3rd ed. London: Elsevier Science Publishing Co Inc, 2022. ISBN 978-0-12-824459-3.

[5] ŠTORK, Jiří. *Dermatovenerologie*. Praha: Galén, 2008. ISBN 978-80-7262-371-6.

[6] VIG, Komal, Atul CHAUDHARI, Shweta TRIPATHI, Saurabh DIXIT, Rajnish SAHU, Shreekumar PILLAI, Vida DENNIS a Shree SINGH. Advances in Skin Regeneration Using Tissue Engineering. *International Journal of Molecular Sciences* [online]. 2017, **18**(4) [cit. 2023-03-31]. ISSN 1422-0067. Available from: doi:10.3390/ijms18040789

[7] GROEBER, Florian, Monika HOLEITER, Martina HAMPEL, Svenja HINDERER a Katja SCHENKE-LAYLAND. Skin tissue engineering — In vivo and in vitro applications. *Advanced Drug Delivery Reviews* [online]. 2011, **63**(4-5), 352-366 [cit. 2023-03-29]. ISSN 0169409X. Available from: doi:10.1016/j.addr.2011.01.005

[8] ČIHÁK, Radomír. *Anatomie* [online]. Třetí, upravené a doplněné vydání. Praha: Grada, 2011-2016 [cit. 2023-03-18]. ISBN 978-80-247-5636-3.

[9] DRAELOS, Zoe Diana a Peter T. PUGLIESE. *Physiology of the skin*. 3rd ed. Carol Stream, IL 60188: Allured Books, 2011. ISBN 9781932633771.

[10] KUSUMA, Shashidhar, Ravi K. VUTHOORI, Melissa PILIANG a James E. ZINS. Skin Anatomy and Physiology. *Plastic and Reconstructive Surgery* [online]. London: Springer London, 2010, 161-171 [cit. 2023-03-21]. ISBN 978-1-84882-512-3. Available from: doi:10.1007/978-1-84882-513-0_13

[11] Epidermis, papillary dermis and reticular dermis. In: *Wikipedia* [online]. 2022 [cit. 2023-04-04]. Available from: https://commons.wikimedia.org/wiki/File:Epidermis,_papillary_dermis_and_reticular_dermis.png

[12] SAKATA, A., K. ABE, K. MIZUKOSHI, T. GOMI a I. OKUDA. Relationship between the retinacula cutis and sagging facial skin. *Skin Research and Technology* [online]. 2018, **24**(1), 93-98 [cit. 2023-03-21]. ISSN 0909752X. Available from: doi:10.1111/srt.12395

[13] WONG, Richard, Stefan GEYER, Wolfgang WENINGER, Jean-Claude GUIMBERTEAU a Jason K. WONG. The dynamic anatomy and patterning of skin. *Experimental Dermatology* [online]. 2016, **25**(2), 92-98 [cit. 2023-03-25]. ISSN 09066705. Available from: doi:10.1111/exd.12832

[14] ZIMOCH, Jakub, Dominika ZIELINSKA, Katarzyna MICHALAK-MICKA, Dominic RÜTSCHE, Roland BÖNI, Thomas BIEDERMANN a Agnes S. KLAR. Bio-engineering a prevascularized human tri-layered skin substitute containing a hypodermis. *Acta Biomaterialia* [online]. 2021, **134**, 215-227 [cit. 2023-03-25]. ISSN 17427061. Available from: doi:10.1016/j.actbio.2021.07.033

[15] Skin. In: *Encyclopædia Britannica* [online]. Encyclopædia Britannica, 2023 [cit. 2023-04-04]. Available from: https://www.britannica.com/science/human-skin#/media/1/547591/2027

[16] Layers of the epidermis. In: *Wikipedia* [online]. 2010 [cit. 2023-04-04]. Available from: https://commons.wikimedia.org/w/index.php?curid=10759438

[17] SORRELL, J. Michael a Arnold I. CAPLAN. Fibroblast heterogeneity: more than skin deep. *Journal of Cell Science* [online]. 2004, **117**(5), 667-675 [cit. 2023-03-27]. ISSN 1477-9137. Available from: doi:10.1242/jcs.01005

[18] KANTA, Jiří. *Collagen matrix as a tool in studying fibroblastic cell behavior* [online]. 2015, **9**(4), 308-316 [cit. 2023-03-27]. ISSN 1933-6918. Available from: doi:10.1080/19336918.2015.1005469

[19] REILLY, David M. a Jennifer LOZANO. Skin collagen through the lifestages: importance for skin health and beauty. *Plastic and Aesthetic Research* [online]. 2021, **8** [cit. 2023-03-27]. ISSN 23479264. Available from: doi:10.20517/2347-9264.2020.153

[20] Collagen - structure, properties and application. *Engineering of Biomaterials* [online]. 2020, (156), 17-23 [cit. 2022-11-15]. ISSN 1429-7248. Available from: doi:https://doi.org/10.34821/eng.biomat.156.2020.17-23

[21] SHOULDERS, Matthew D. a Ronald T. RAINES. Collagen Structure and Stability. *Annual Review of Biochemistry* [online]. 2009, **78**(1), 929-958 [cit. 2023-03-27]. ISSN 0066-4154. Available from: doi:10.1146/annurev.biochem.77.032207.120833

[22] SCHRÄDER, Christoph U., Andrea HEINZ, Petra MAJOVSKY, Berin KARAMAN MAYACK, Jürgen BRINCKMANN, Wolfgang SIPPL a Christian E.H. SCHMELZER. Elastin is heterogeneously cross-linked. *Journal of Biological Chemistry* [online]. 2018, **293**(39), 15107-15119 [cit. 2023-03-27]. ISSN 00219258. Available from: doi:10.1074/jbc.RA118.004322

[23] MUIZNIEKS, Lisa D., Anthony S. WEISS a Fred W. KEELEY. Structural disorder and dynamics of elastin. *Biochemistry and Cell Biology* [online]. 2010, **88**(2), 239-250 [cit. 2023-27-3]. ISSN 0829-8211. Available from: doi:10.1139/O09-161

[24] RODGERS, Ursula R. a Anthony S. WEISS. Cellular interactions with elastin. *Pathologie Biologie* [online]. 2005, **53**(7), 390-398 [cit. 2023-03-27]. ISSN 03698114. Available from: doi:10.1016/j.patbio.2004.12.022

[25] SHI, Donglu, ed. *Biomaterials and Tissue Engineering*. 1. Berlin: Springer, 2004. ISBN 3540222030.

[26] BAKHSHANDEH, Behnaz, Payam ZARRINTAJ, Mohammad Omid OFTADEH, Farid KERAMATI, Hamideh FOULADIHA, Salma SOHRABI-JAHROMI a Zarrintaj ZIRAKSAZ. Tissue engineering; strategies, tissues, and biomaterials. *Biotechnology and Genetic Engineering Reviews* [online]. 2017, **33**(2), 144-172 [cit. 2023-03-28]. ISSN 0264-8725. Available from: doi:10.1080/02648725.2018.1430464

[27] GODBEY, W. T. a A. ATALA. In Vitro Systems for Tissue Engineering. *Annals of the New York Academy of Sciences* [online]. 2002, **961**(1), 10-26 [cit. 2023-03-28]. ISSN 00778923. Available from: doi:10.1111/j.1749-6632.2002.tb03041.x

[28] BÖTTCHER-HABERZETH, Sophie, Thomas BIEDERMANN a Ernst REICHMANN. Tissue engineering of skin. *Burns* [online]. 2010, **36**(4), 450-460 [cit. 2023-03-29]. ISSN 03054179. Available from: doi:10.1016/j.burns.2009.08.016

[29] GOODARZI, Parisa, Khadijeh FALAHZADEH, Mehran NEMATIZADEH, Parham FARAZANDEH, Moloud PAYAB, Bagher LARIJANI, Akram TAYANLOO BEIK

a Babak ARJMAND. Tissue Engineered Skin Substitutes. *Cell Biology and Translational Medicine, Volume 3* [online]. Cham: Springer International Publishing, 2018, 143-188 [cit. 2023-03-29]. Advances in Experimental Medicine and Biology. ISBN 978-3-030-04184-7. Available from: doi:10.1007/5584_2018_226

[30] WEI, Chao, Yihua FENG, Dezhao CHE, Jiahui ZHANG, Xuan ZHOU, Yanbin SHI a Li WANG. Biomaterials in skin tissue engineering. *International Journal of Polymeric Materials and Polymeric Biomaterials* [online]. 2022, **71**(13), 993-1011 [cit. 2023-03-30]. ISSN 0091-4037. Available from: doi:10.1080/00914037.2021.1933977

[31] STARK, Hans-Jürgen, Axel SZABOWSKI, Norbert E. FUSENIG a Nicole MAAS-SZABOWSKI. Organotypic cocultures as skin equivalents: A complex and sophisticated in vitro system. *Biological Procedures Online* [online]. 2004, **6**(1), 55-60 [cit. 2023-05-12]. ISSN 1480-9222. Available from: doi:10.1251/bpo72

[32] GARROD, Mathew a David Yi San CHAU. *An Overview of Tissue Engineering as an Alternative for Toxicity Assessment* [online]. 2016, **19**(1), 31-71 [cit. 2023-05-12]. ISSN 1482-1826. Available from: doi:10.18433/J35P6P

[33] BALLS, Michael. Are Animal Tests Inherently Valid?. *Alternatives to Laboratory Animals* [online]. 2004, **32**(1), 755-758 [cit. 2023-05-12]. ISSN 0261-1929. Available from: doi:10.1177/026119290403201s125

[34] BOEHNKE, Karsten, Nicolae MIRANCEA, Alessandra PAVESIO, Norbert E. FUSENIG, Petra BOUKAMP a Hans-Jürgen STARK. Effects of fibroblasts and microenvironment on epidermal regeneration and tissue function in long-term skin equivalents. *European Journal of Cell Biology* [online]. 2007, **86**(11-12), 731-746 [cit. 2023-05-12]. ISSN 01719335. Available from: doi:10.1016/j.ejcb.2006.12.005

[35] SRIRAM, Gopu, Paul Lorenz BIGLIARDI a Mei BIGLIARDI-QI. Fibroblast heterogeneity and its implications for engineering organotypic skin models in vitro. *European Journal of Cell Biology* [online]. 2015, **94**(11), 483-512 [cit. 2023-05-10]. ISSN 01719335. Available from: doi:10.1016/j.ejcb.2015.08.001

[36] OH, Ji Won, Tsai-Ching HSI, Christian Fernando GUERRERO-JUAREZ, Raul RAMOS a Maksim V. PLIKUS. Organotypic Skin Culture. *Journal of Investigative Dermatology* [online]. 2013, **133**(11), 1-4 [cit. 2023-05-16]. ISSN 0022202X. Available from: doi:10.1038/jid.2013.387

[37] DIEKMANN, Johanna, Lirija ALILI, Okka SCHOLZ, Melanie GIESEN, Olaf HOLTKÖTTER a Peter BRENNEISEN. A three-dimensional skin equivalent reflecting some aspects of in vivo aged skin. *Experimental Dermatology* [online]. 2016, **25**(1), 56-61 [cit. 2023-05-16]. ISSN 09066705. Available from: doi:10.1111/exd.12866

[38] JANG, Hye-Jeong, Jung Bok LEE a Jeong-Kee YOON. Advanced In Vitro Three-Dimensional Skin Models of Atopic Dermatitis. *Tissue Engineering and Regenerative Medicine* [online]. 2023 [cit. 2023-05-16]. ISSN 1738-2696. Available from: doi:10.1007/s13770-023-00532-1

[39] BELLO, Ysabel M., Anna F. FALABELLA a William H. EAGLSTEIN. Tissue-Engineered Skin. *American Journal of Clinical Dermatology* [online]. 2001, **2**(5), 305-313 [cit. 2023-05-15]. ISSN 1175-0561. Available from: doi:10.2165/00128071-200102050-00005

[40] SALTZMAN, W. Mark. *Tissue engineering : engineering principles for the design of replacement organs and tissues*. Oxford: Oxford University Press, 2004. ISBN 978-0-19-514130-6.

[41] HOFMANN, Elisabeth, Anna SCHWARZ, Julia FINK, Lars-Peter KAMOLZ a Petra KOTZBECK. Modelling the Complexity of Human Skin In Vitro. *Biomedicines* [online]. 2023, **11**(3) [cit. 2023-05-16]. ISSN 2227-9059. Available from: doi:10.3390/biomedicines11030794

[42] GANGATIRKAR, Pradnya, Sophie PAQUET-FIFIELD, Amy LI, Ralph ROSSI a Pritinder KAUR. Establishment of 3D organotypic cultures using human neonatal epidermal cells. *Nature Protocols* [online]. 2007, **2**(1), 178-186 [cit. 2023-05-10]. ISSN 1754-2189. Available from: doi:10.1038/nprot.2006.448

[43] *Human skin equivalent as an alternative to animal testing - Scientific Figure on ResearchGate* [online]. In: . [cit. 2023-05-17]. Available from: https://www.researchgate.net/figure/Histological-cross-section-of-human-skin-and-of-the-three-dimensional-skin-equivalent_fig1_41761599

[44] CAI, Runxuan, Naroa GIMENEZ-CAMINO, Ming XIAO, Shuguang BI a Kyle A. DIVITO. Technological advances in three-dimensional skin tissue engineering. *REVIEWS ON ADVANCED MATERIALS SCIENCE* [online]. 2023, **62**(1) [cit. 2023-05-17]. ISSN 1605-8127. Available from: doi:10.1515/rams-2022-0289

[45] ASSANGA, Iloki. Cell growth curves for different cell lines and their relationship with biological activities. *International Journal of Biotechnology and Molecular Biology Research* [online]. 2013, **4**(4), 60-70 [cit. 2022-10-29]. ISSN 2141-2154. Available from: doi:10.5897/IJBMBR2013.0154

[46] THEOCHARIS, Achilleas D., Spyros S. SKANDALIS, Chrysostomi GIALELI a Nikos K. KARAMANOS. Extracellular matrix structure. *Advanced Drug Delivery Reviews* [online]. 2016, **97**, 4-27 [cit. 2022-10-29]. ISSN 0169409X. Available from: doi:10.1016/j.addr.2015.11.001

[47] FRESHNEY, R. Ian. Basic Principles of Cell Culture. *Culture of Cells for Tissue Engineering* [online]. Hoboken, NJ, USA, 2005, 1-22 [cit. 2022-11-12]. ISBN 9780471741817. Available from: doi:10.1002/0471741817.ch1

[48] BOBADILLA, Ana Victoria Ponce, Jazmine ARÉVALO, Eduard SARRÓ et al. In vitro cell migration quantification method for scratch assays. *Journal of The Royal Society Interface* [online]. 2019, **16**(151) [cit. 2022-12-03]. ISSN 1742-5689. Available from: doi:10.1098/rsif.2018.0709

[49] MAK, Michael, Fabian SPILL, Roger D. KAMM a Muhammad H. ZAMAN. Single-Cell Migration in Complex Microenvironments: Mechanics and Signaling Dynamics. *Journal of Biomechanical Engineering* [online]. 2016, **138**(2) [cit. 2022-12-04]. ISSN 0148-0731. Available from: doi:10.1115/1.4032188

[50] VANG MOURITZEN, Michelle a Håvard JENSSEN. Optimized Scratch Assay for In Vitro Testing of Cell Migration with an Automated Optical Camera. *Journal of Visualized Experiments* [online]. 2018, (138) [cit. 2022-12-04]. ISSN 1940-087X. Available from: doi:10.3791/57691

[51] LIANG, Chun-Chi, Ann Y PARK a Jun-Lin GUAN. In vitro scratch assay: a convenient and inexpensive method for analysis of cell migration in vitro. *Nature Protocols* [online]. 2007, **2**(2), 329-333 [cit. 2022-12-04]. ISSN 1754-2189. Available from: doi:10.1038/nprot.2007.30

[52] LIN, Jin-Young, Kai-Yin LO a Yung-Shin SUN. Effects of Substrate-Coating Materials on the Wound-Healing Process. *Materials* [online]. 2019, **12**(17) [cit. 2022-12-04]. ISSN 1996-1944. Available from: doi:10.3390/ma12172775

[53] Coating Protocols for ibidi Labware. In: *Ibidi* [online]. 2022 [cit. 2023-05-10]. Available from: https://ibidi.com/img/cms/support/AN/AN08_Coating.pdf

[54] Collagen coating protocol. In: *Neuvitro corporation* [online]. [cit. 2023-05-10]. Available from: https://www.neuvitro.com/collagen-coating-protocol

[55] Collagen Attachment Protocols, Solubility, and Stability. In: *Merck* [online]. [cit. 2023-05-10]. Available from: https://www.sigmaaldrich.com/CZ/en/technical-documents/technical-article/cell-culture-and-cell-culture-analysis/mammalian-cell-culture/collagen-product-protocols

[56] STACEY, Glyn N. Cell Culture Contamination. *Cancer Cell Culture* [online]. Totowa, NJ: Humana Press, 2011, 79-91 [cit. 2023-05-10]. Methods in Molecular Biology. ISBN 978-1-61779-079-9. Available from: doi:10.1007/978-1-61779-080-5_7

LIST OF ABBREVIATIONS

µg micrograms

µl, μl^{-1} microliters

µm micrometers

2D Two-dimensional

3D Three-dimensional, trojrozměrný

Ala Alanine

ALI Air-Liquid Interface

BME Basal Medium Eagle

CEA Cultured Epidermal Autograft

cm^{-2} Centimeters squared

Collagen A Bovine collagen type I

Collagen B Collagen type I solution from rat tail

Collagen C Rat tail collagen coating solution

Collagen D Collagen type I, high concentration, Rat Tail

DMEM Dulbecco's Modified Essential Medium

ECM Extracellular matrix

FBS Fetal Bovine Serum

FCS Calf Serum

g grams

GAG Glycosaminoglycan

Gly Glycine

h hours

HDF Human Neonatal Dermal Fibroblasts

HEK Human Neonatal Epidermal Keratinocytes

HSE Human Skin Equivalent

Hyp Hydroxyproline

ITS Insulin-transferrin-selenium

KGM2 Keratinocyte Growth Medium 2

Ly Lysine

M Molarity

m^2 meters squared

mg miligrams

ml, ml^{-1} mililiters

mm milimeters

mm^2 milimiters squared

OCS Organotypic Culture System

OEP Octaethylporphyrin

PBS Dulbecco's Phosphate Buffered Saline

PDT Population Doubling Time

pH potential of hydrogen

Pro Proline

RPM Rotations Per Minute

T3 Triiodothyronine

TE Tissue engineering

Tel Tropoelastin

UPW Ultra-pure Water

Val Valine

LIST OF FIGURES

LIST OF TABLES